Reflective Light-Curves of Ellipsoidally-Shaped Outer Solar-System Objects and Exoplanets

M.W. Beekman
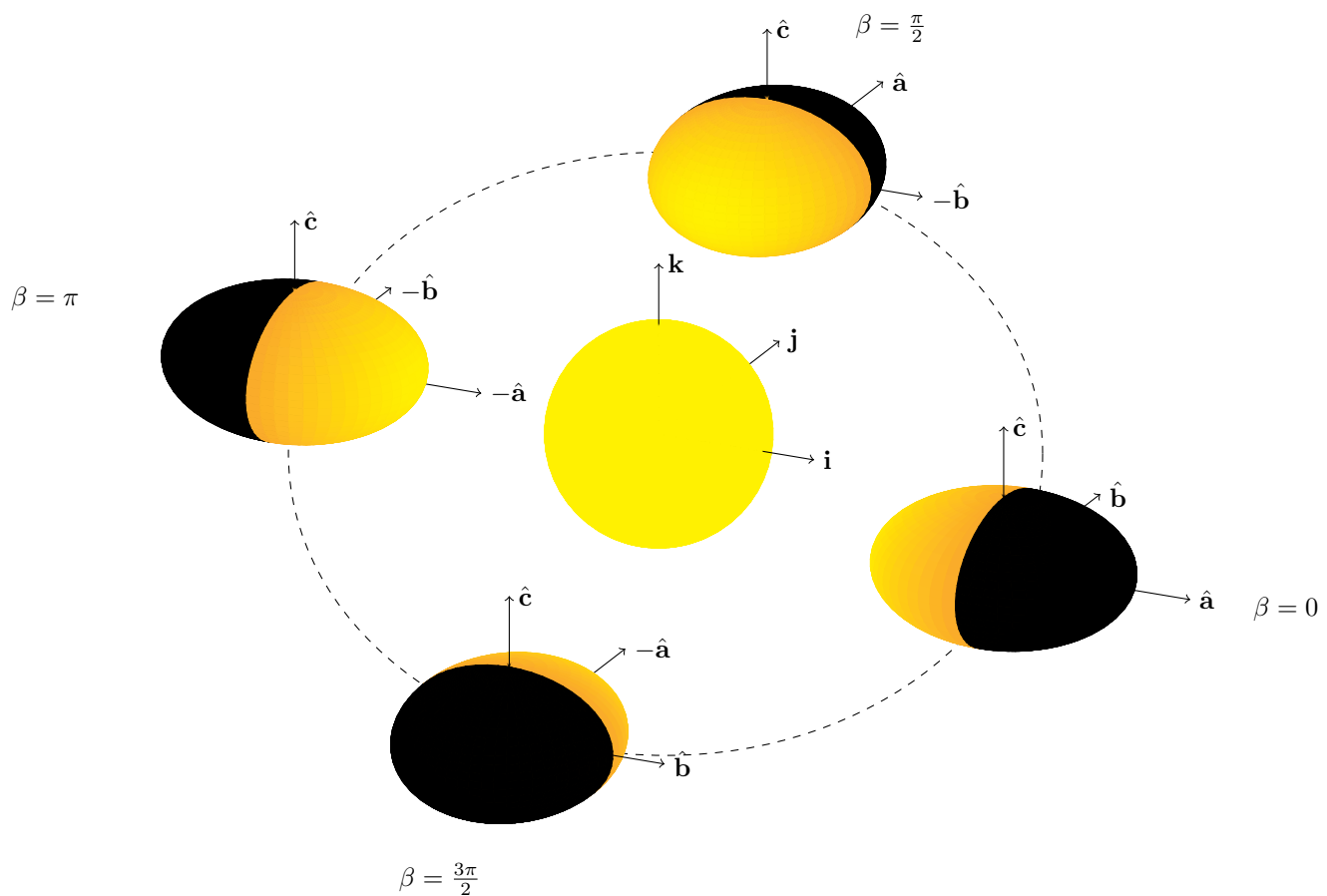
Abstract

In this thesis we consider reflective light-curves of planets, graphs of the intensity of the light originating from the parent star that the planet reflects versus time. In almost all instances, planets are modelled as spheres, like in [1] and [2]. However, planets are better approximated by ellipsoids as proved by Isaac Newton in the Principia [3]. In our own solar system, we can observe that planets are not spheres when we look at for example Jupiter [4] and Haumea [5]. We study the effect on the light-curve of the change from a spherical to an ellipsoidal model.

For example, a spherical model of a homogeneous planet at edge-on observation would predict a constant light-intensity during one rotation around its axis due to the symmetry of the model. Note that we assumed here that the planet sits approximately still in the sky during one rotation around its axis. However, an ellipsoidal model of a homogeneous planet at edge-on observation would predict a variable light-intensity. [5] shows a difference between the maximum and the minimum value of the measured light-curve of Haumea of 0.32 magnitudes. This shows that an ellipsoidal model has a significant effect on the light-curve. Furthermore, in contrast to the spherical model, with the light-curves for the ellipsoidal model we can for example calculate the spin of the planet in certain cases, which makes them more interesting. By calculating the light-curve with the ellipsoidal model, we can determine the shape of planets and therefore gain knowledge about the internal structure of planets.

Where others, like [5], have calculated the light-curve for an ellipsoidally-shaped planet numerically, we calculate them analytically. We accomplish this with the analytical equation of the light-curve postulated by [6]. We assume that planets have a homogeneous reflecting surface, we assume parallel incident light-rays, we assume Lambertian reflection and we assume that the planet is in a circular orbit around its parent star. We did not calculate the light-curves for non-circular orbits. However, the results can easily be modified to include elliptical Kepler orbits since the light-curve depends linearly on the orbital radius. We consider the applications of a solar system triaxially-shaped planet, like Haumea, a spheroidally-shaped exoplanet and a tidally-locked, triaxially-shaped exoplanet. We considered both edge-on and face-on observation.

We confirmed the dimensions given by [5] for the dwarf planet Haumea. We found that for a given tilt of the planet's rotation axis, there are enough measurable Fourier coefficients to determine the dimensions of the planet in each of our applications. The only exception we found is a spheroidally-shaped exoplanet at edge-on observation without tilt. In that case, we do not have enough information to differentiate between the flattening and the size of the exoplanet.

Contents

Nomenclature

Angles

β Orbital phase

δ Azimuthal angle of $\hat{\mathbf{n}}$

γ Polar angle of $\hat{\mathbf{n}}$

ϕ Azimithal angle of $\hat{\mathbf{u}}$

θ Polar angle of $\hat{\mathbf{u}}$

Constants

κ_1, κ_2 First and second principal curvature constants

K Gaussian curvature constant

$(\mathbf{i}, \mathbf{j}, \mathbf{k})$ Basis

(x, y, z) Coordinates in principal axes $\mathbf{a}$, $\mathbf{b}$ and $\mathbf{c}$

$\mathbf{a}, \mathbf{b}, \mathbf{c}$ The semi-principal axes of the ellipsoid

Fourier coefficients

$a_i, i \in \{\mathbb{N} \cup \{0\}\}$ i^{th} cosine Fourier coefficient

$b_i, i \in \mathbb{N}$ i^{th} sine Fourier coefficient

Matrices

A The positive definite matrix containing all the information about the shape of the ellipsoid

A_{jk} A in sequence rotated around $\mathbf{j}$ and $\mathbf{k}$

A_{sjk} A in sequence rotated around $\hat{\mathbf{n}}$, $\mathbf{j}$ and $\mathbf{k}$

A_s A rotated around $\hat{\mathbf{n}}$

$R_{\mathbf{j}}(\gamma)$ Rotation matrix around $\mathbf{j}$ with phase γ

$R_{\mathbf{k}}(\delta)$ Rotation matrix around $\mathbf{k}$ with phase δ

$R_s(\beta)$ Rotation matrix around $\hat{\mathbf{n}}$ with phase β

Properties of celestial bodies

Ω Planetary rotational frequency

ω Orbtial rotational frequency

r Star radius

s Maximum length of $\mathbf{s}$ perpendicular to $\mathbf{R}$

Sets

Φ	Integration bound for ϕ
$\supset$	Illuminated area of the planet's surface the observer can see
$\mathbf{S}$	Surface of an ellipsoid
S_o	Observed area of the planet's surface
S_r	Illuminated area of the planet's surface

Vectors

$\hat{\mathbf{n}}$	Planetary spin axis
$\mathbf{o}$	Vector from the centre of the planet to the observer
$\mathbf{R}$	Vector from the centre of the parent star to the centre of the planet
$\mathbf{s}$	Surface vector of an ellipsoid
$\mathbf{u}$	Vector normal to the ellipsoidal surface at $\mathbf{s}$

Other symbols

f	Equation for the light-curve
t	Time

1.   Introduction

In this thesis, we consider outer solar-system-objects and exoplanets. Exoplanets are planets located outside our solar system. The first exoplanet was detected in 1989, but was confirmed much later in 2002 [7]. This exoplanet was detected by the means of radial velocity. Radial velocity is the method of detecting variations in the velocity of a star relative to earth with for example the Doppler effect. These variations in velocity can sometimes be attributed to orbiting planets [8].

In 1992, the first three exoplanets were confirmed. These exoplanets where found with pulsar timing, an example of a timing method [7]. Planets can have a measurable effect on periodic phenomena of nearby objects. Timing methods are based on measuring variations in the period of these phenomena, indicating a nearby object. Other examples of timing methods are transit timing and eclipsing binary minima timing. In this case, the gravitational pull of these exoplanets influenced the motion of their parent star, a pulsar. Due to these planets, the time between the pulses of the pulsar varied. Also because of these planets, the frequency of the pulses varied due to Doppler shift [8].

At the present, a grand total of 3472 exoplanets have been discovered and confirmed. The large majority of these exoplanets, 2650 of them, have been found with transit photometry [9]. Transit photometry is observing a drop in the visual brightness of a star that is caused by an exoplanet that transits in front of the star. The brightness of the star OGLE-TR-56 in apparent magnitudes against time in days is shown in figure 1. Here you can see a dip in the brightness after one day, indicating an orbiting planet, OGLE-TR-56b, with an orbital period of 1.21190 days [10].
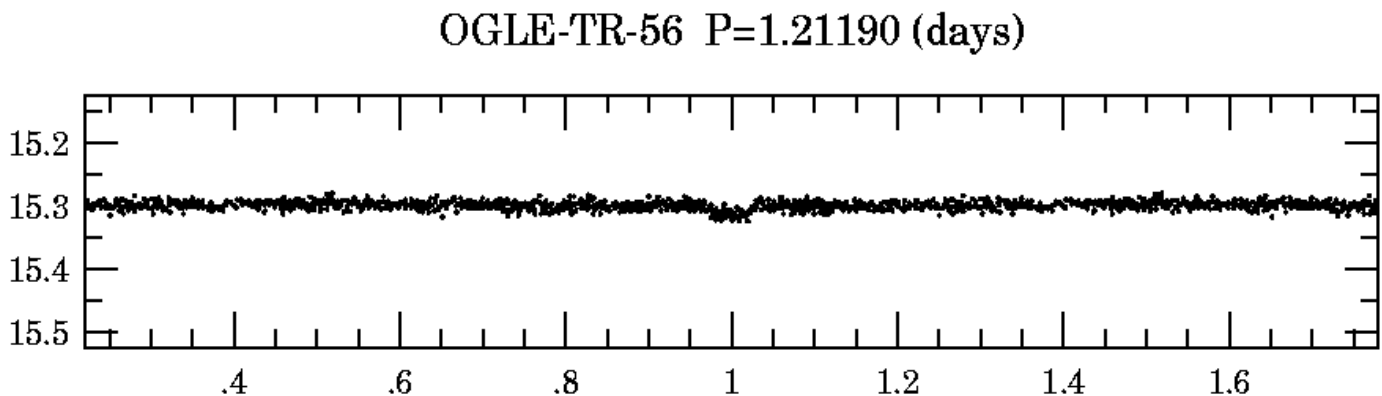
Figure 1: The brightness of the star OGLE-TR-56 in apparent magnitudes against time in days. Here you can see a dip in the brightness after one day, indicating the orbiting planet, OGLE-TR-56b, with an orbital period of 1.21190 days [10].

The method of imaging we study in this thesis is direct imaging. Radial velocity, timing methods, transit photometry and gravitational lensing are examples of indirect detection. With direct imaging, we observe the light originating from or reflected off the planet. With indirect detection, we observe the light originating from another body and search for the effects of a planet on that light. Most of the indirect detection like radial velocity, timing methods and transit photometry detect a change in the light emitted by the parent star of the exoplanet. Gravitational lensing however does not detects the light of the parent star, but from a source star as shown in figure 2. We can detect the planet as starlight from a source star is bend differently by a lens star with and without a planet in its orbit.
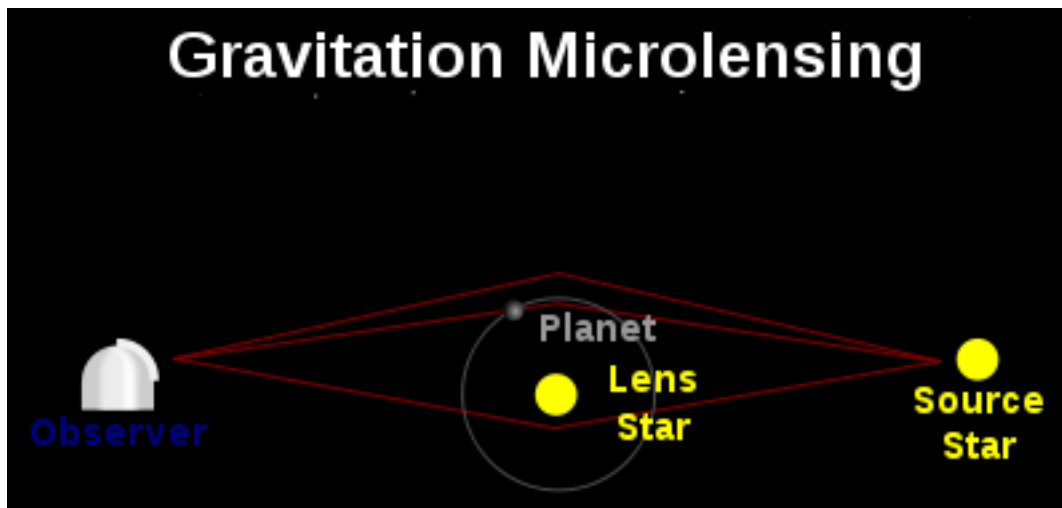
Figure 2: Starlight from a source star bend by gravitational lensing of the lens star and a orbiting planet towards an observer.

Planets are extremely faint compared to their parent stars, which makes direct imaging far more difficult to achieve in comparison with indirect detection. Therefore, only 70 exoplanets have been found with direct imaging at the present [9]. Also, the first confirmed discovery with direct imaging was as late as 2014, namely the exoplanet 2M1207b. This was possible due to a combination of its large orbital radius of 40 AU, the relatively faint parent-star, a brown dwarf that is only 100 times brighter than the exoplanet, because of the relatively great size of the exoplanet, several times larger than Jupiter, and because of the high temperature of the planet [11].

With the method of direct imaging, we cannot achieve detailed images of exoplanets as even the nearest exoplanet is at a distance of 4.36 light years from Earth [12]. Even for distant objects in our solar system and with our most powerful telescopes at the present, a planet is smaller than the size of a pixel. Therefore, astronomers measure the time-dependent intensity of light which originates from the planet. We call this graph the light-curve [13].
The light-intensity of planets are extremely faint in comparison to the light-intensity of their parent stars. For example, take a spherically-shaped Jupiter size planet, the largest planet in our solar system, in the orbit of Mercury around our sun, the planet with the orbit closest to the sun, that reflects all the light it receives. Then the light from the planet would be less that of the cross section of the planet that reflects all the light towards the observer, $\pi r^2/4\pi R^2$, where r is the radius of Jupiter, 69.173 kilometres [14], and R is the orbital radius of Mercury, 0.387 AU [14]. Even then, the light that the planet reflects would be at least 2.8 million times fainter than the light of our Sun when the Sun is at the same distance from the observer as the planet.
An example of a large planet in close orbit is HAT-P-7b, with a radius of 1.3363 times the radius of Jupiter at an orbital radius of only 0.0377 AU. But even HAT-P-7b is still 10^4 fainter than its parent star.

Even if we only have the light-curve at our disposal, we occasionally can still determine many properties of a planet:

1. We can use the period of the light-curve to determine the rotational period of the planet. Note that we can not determine the rotational period if the planet is homogeneous and symmetrical around its rotational axis for some observer orientations.

2. We can determine the shape of a planet when we look at one rotational period of the planet for some

observer orientations. For example, as aforementioned, we can determine if the planet is symmetrical around its rotation axis.

3. We can determine the orbit of a planet. We determine that with the reflective light-curve, the time-dependent intensity of the light that is reflected from the sun towards the observer. The reflective light-curve depends on the apparent magnitude of the parent-star which in turn depends on the distance between the planet and its parent-star. That is, with the reflective light-curve we can determine the orbital radius over time, the orbit. Note that this is only possible if we know the albedo and the size of the planet in question.

4. If the albedo is known, we can obtain a rough estimate of the size of the planet with the reflective light-curve by comparing the reflective light-curve to the apparent magnitude of the star the planet orbits.

5. We can, up to a point, determine the albedo of the reflective surface of the planet. We can determine this by noticing differences between the measured light-curve and the calculated light-curve of a homogeneous planet over a single rotational period. If we detect changes between multiple rotational periods, it could indicate that the planet has an atmosphere.

Isaac Newton proved in the Principia that a rotating self-gravitating fluid body in equilibrium takes the form of an oblate ellipsoid [3]. Only in extreme cases, near the Roche limit, this is not a good approximation due to the tidal forces of a nearby body almost as strong as the gravity of the planet at its surface. In [15] is shown that ellipsoids are triaxial for fast spinning planets. Moreover, in our own solar system, we can observe that planets are not spheres when we look at for example Jupiter [4] and Haumea [5]. Although most planets are ellipsoidally-shaped, the predominate model used when analytically calculating light-curves is the spherical model. Examples are [1] and [2]. Others, like [5], have calculated the light-curve for an ellipsoidally-shaped planet, but numerically. We calculate the light-curve of ellipsoidally-shaped planets analytically. Note that an ellipsoidal model is always more accurate in calculating light-curves than the spherical model, since a sphere is just a special case of an ellipsoid.

We primarily consider exoplanets, but our method also gives rise to applications within our solar system. An example we consider is the rapidly spinning triaxially-shaped dwarf planet Haumea [16]. This method could also have applications for the recently discovered Planet Nine [17] or other Kuiper Belt objects.

In this thesis, we calculate the reflective light-curve. We do not consider thermal light-curves. These are light-curves of the thermal radiation the planet gives off itself. As we discussed, reflective light-curves can give us information about, among other properties, the shape of the planet.
Reflective light-curves are difficult to calculate as we have to take the surface of the star and the surface of the planet into account.
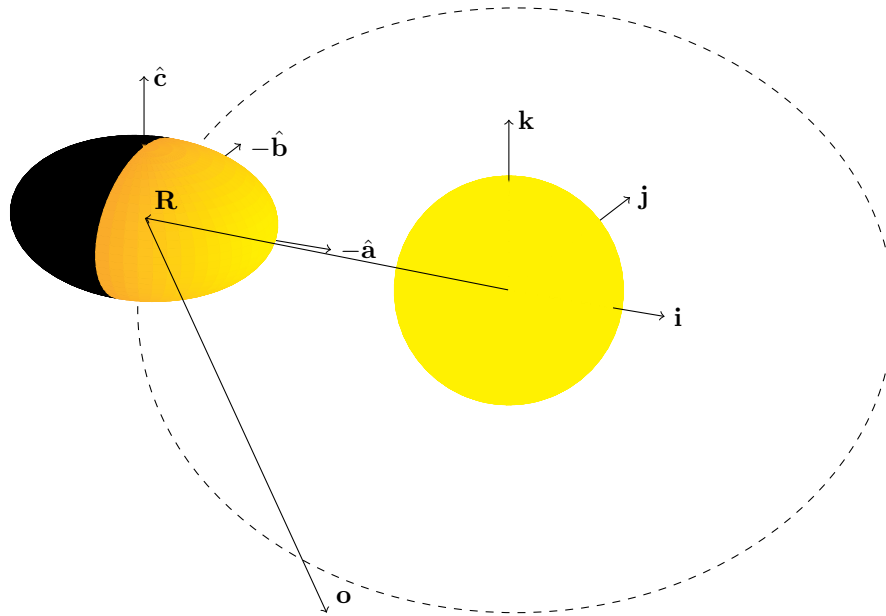
Figure 3: An ellipsoid orbiting a star with the light-rays of the starlight following the vectors **R** and **o**.

In [6], an analytic equation of the light-curve for ellipsoidally-shaped planets has been derived. Our goal is to try to determine the shape of a planet with this equation of the light-curve. To that end, we make a few assumptions and approximations. We assume that

1. planets are perfect ellipsoids. We have already argued that planets are ellipsoidally-shaped. However, now we assume that planets are smooth. This is a good approximation as the popular expression, "If we shrunk the Earth down to the size of a billiard ball, it would be smoother than an actual billiard ball", illustrates.

2. the planet is in a circular orbit around its parent star. This is true for close-in planets that are ellipsoidally-shaped due to tidal deformation. If a planet is ellipsoidally-shaped due to for example spin, like Haumea, their orbit is generally not circular. We did not calculate the light-curves for non-circular orbits. However, the results can easily be modified to include elliptical Kepler orbits since the light-curve is linearly depended on the orbital.

3. the reflection on the reflective surface of the planet is Lambertian. This is a good assumption for rough surfaces and for thick atmospheres [18].

4. the reflective surface of the planet is homogeneous with an surface albedo of 1. The surface albedo of planets is always smaller than 1, but this affects the light-curve linearly. In other words, this does not effect the calculation of the shape of the planet, only the size. For the low contrast images we have of exoplanets, surface details are not visible. So for these applications, a homogeneous surface is a good approximation. However in chapter 3 we will see that we can detect that the dwarf planet Haumea has a different albedo on its two sides.

5. the starlight that falls on the planet's reflective surface follows **R**, the vector from the centre of the parent star to the centre of the planet as seen in figure 3. This is a reasonable approximation for planets like Earth. As the diameter of our sun, r, is 1.391.400 kilometres [19] and the minimal distance from the earth to the sun, R, is 147.095.000 kilometres [20], the maximum angle possible between the light of opposite sides of the sun is only 0.54 degrees. With s the maximum radius of

the planet and r the radius of its parent star, this approximation is accurate for $R \gg r + s$. With this assumption it is not necessary to take the stellar surface into account.

6. the starlight reflected off the planet follows **o**, the vector from the centre of the planet to the observer as seen in figure 3. That is, for the observer, the planet is a point source. With the nearest planetary system Alpha Centauri being at a distance of 4.36 light years [12] and the largest exoplanet discovered so far, HD 100546 b, has a diameter of 3.2 light seconds [21], this is a very good approximation for exoplanets. This is also a good approximation for distant solar-system objects. In our example of Haumea in section 3., we see that the distant from the observer to Haumea of 30.64AU is more than 10^6 times greater than 1920 kilometres, the lenght of the largest semi-principal axis of Haumea.

7. **o** is a constant vector. This is a good approximation for exoplanets as the distance that an observer on Earth for example and the observed planet travels is far less than the distance between the observer and the observed planet. This is because the largest known orbit of a planet around a single star is about 650 astronomical units [22] and the orbit of the Earth is only 1 astronomical unit [20], while the nearest planetary system Alpha Centauri is at a distance of 4.36 light years [12].

In section 2, we use the work of [6] to derive the equation of the light-curves of ellipsoidally-shaped planets. We apply this equation for the light-curve in section 3 to the case of a solar system triaxially-shaped dwarf planet, in section 4 to the case of a spheroidally-shaped exoplanet and in section 5 to the case of a tidally-locked, triaxially-shaped exoplanet. In section 6 we discuss the results of section 3 through 5. In sections 7 and 8 we derive some useful results contrived by Paul Visser to support section 2. Finally, in section 9 we show the MATLAB [23] scripts used in sections 3 through 5.

2. Derivation of light-curve from ellipsoidally-shaped planets

2.1. Describing ellipsoidally-shaped planets

To determine the light-curve we first look at the reflective surface of the planet in the shape of an ellipsoid. The surface of an ellipsoid abides:

$$\frac{x^2}{a^2} + \frac{y^2}{b^2} + \frac{z^2}{c^2} = 1, \tag{1}$$

where x, y and z are respectively the coördinates co-rotating with the planet. We denote the principal axes $\mathbf{a}, \mathbf{b}$ and $\mathbf{c}$. We define the positive-definite matrix

$$A = \begin{pmatrix} a^{-2} & 0 & 0 \\ 0 & b^{-2} & 0 \\ 0 & 0 & c^{-2} \end{pmatrix}.$$

We write for a surface vector

$$\mathbf{s} = \begin{pmatrix} x \\ y \\ z \end{pmatrix}.$$

Now we can rewrite equation 1 to

$$\mathbf{s}^T A \mathbf{s} = 1. \tag{2}$$

We define the surface of the planet as all the surface vectors satisfying equation 2

$$\mathbf{S} = \left\{ \mathbf{s} | \mathbf{s}^T A \mathbf{s} = 1 \right\}.$$

In order to calculate the amount of light from the parent star that gets reflected in the direction of the observer, we define $\mathbf{u}$, the vector normal to the ellipsoidal surface at $\mathbf{s}$. The coordinate system of an ellipsoidally-shaped planet for one possible $\mathbf{s} \in \mathbf{S}$ is shown in figure 4.
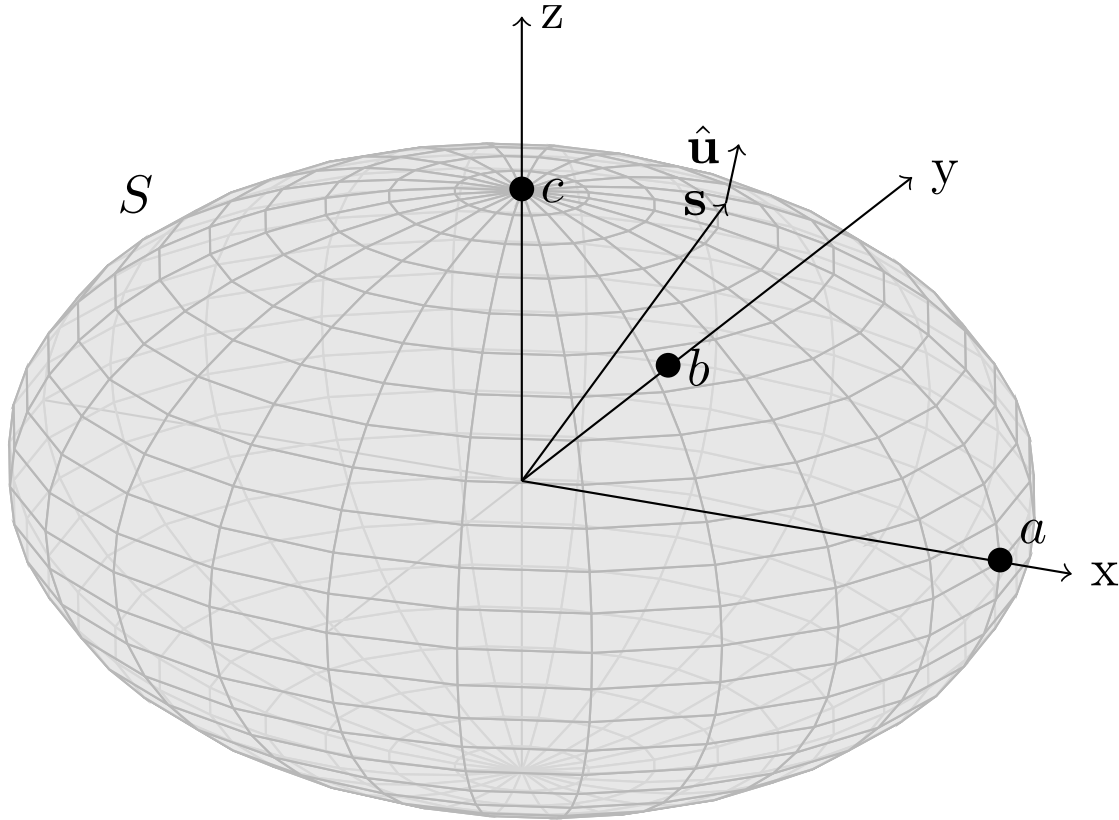
Figure 4: Coordinate system of an ellipsoidally-shaped planet for one possible $\mathbf{s} \in \mathbf{S}$.

As a normal, $\mathbf{u}$ is in the direction of $\nabla\left(\mathbf{s}^T A \mathbf{s}\right) = 2A\mathbf{s}$. We set $\mathbf{u} = A\mathbf{s}$, which is equivalent to $\mathbf{s} = A^{-1}\mathbf{u}$. Here we can justify losing the factor of 2, as we are only interested in the direction of $\mathbf{u}$.
In order to write $\mathbf{s}$ in terms of $\hat{\mathbf{u}}$, we calculate the length of $\mathbf{u}$

$$u^2 = |\mathbf{u}|^2 = \mathbf{u}^T\mathbf{u} = \mathbf{s}^T A^2 \mathbf{s} = \left|A^{-1/2}\hat{\mathbf{u}}\right|^{-2}.$$

From this calculation follows that the unit normal $\hat{\mathbf{u}}$ is given by

$$\hat{\mathbf{u}} = \frac{A\mathbf{s}}{|A\mathbf{s}|},$$

with the inverse relation

$$\mathbf{s} = \frac{A^{-}1\hat{\mathbf{u}}}{|A^{-1/2}\hat{\mathbf{u}}|}.$$

In some applications, as we will see in chapter 3, there is not enough information to find the dimensions of an ellipsoid. In [15] we find tables that relate b/a to c/a for Jacobi ellipsoids. With this relation, we only need two measurable variables to find the three variables a, b and c.
In figure 5 we show a diagram of equatorial bulging against polar flattening [6] of Maclaurin spheroids and Jacobi ellipsoids. Maclaurin spheroids and Jacobi ellipsoids are the equilibrium solution of a spinning body of constant density under self-gravity. Shown are some level curves for different ratios between the mass of the planet and the mass of the parent star.
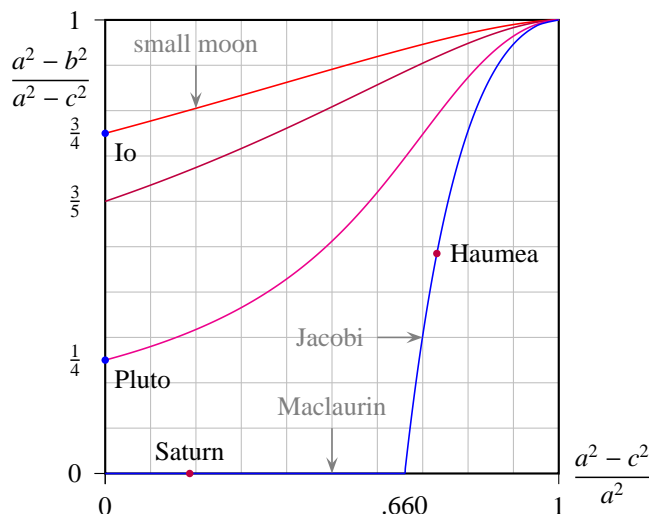
Figure 5: The curve for Jacobi ellipsoids that relate b/a to c/a [6]. Also shown is the curve for Maclaurin spheroids.

With this diagram, we will be able to determine the dimensions of Haumea approximated by a Jacobi ellipsoid.

2.2. Derivation of the light-curve

Now we are going to draft the equation for the light-curve. Let $\hat{\mathbf{o}}$ and $\hat{\mathbf{R}}$ be respectively the unity vectors from the centre of the planet to the observer and from the star the planet orbits to the centre of the planet. Where $\hat{\mathbf{o}}$ is taken as a constant vector throughout this thesis, $\hat{\mathbf{R}}$ may be time-dependent due to the orbit of the planet around it's parent star. Let $\mathbf{S}_r = \{\mathbf{s} \in \mathbf{S} | \mathbf{s} \cdot \mathbf{R} < 0\}$, the surface of the planet that receives light from the star and $\mathbf{S}_o = \{\mathbf{s} \in \mathbf{S} | \mathbf{s} \cdot \mathbf{o} > 0\}$, the surface of the planet that can be seen by the observer. The light we receive comes only from the *lune* $\mathbb{D} = \mathbf{S}_r \cap \mathbf{S}_o$, the illuminated part of the planet the observer can see.

The light-curve is then given by [6]

$$f(t) = \frac{4}{\pi} \int \int_{\mathbb{D}} \frac{\mathrm{d}^2\mathbf{s}}{|\mathbf{R}|^2} \left(-(\hat{\mathbf{R}} \cdot \hat{\mathbf{u}})(\hat{\mathbf{u}} \cdot \hat{\mathbf{o}}) \right), \tag{3}$$

the surface integral over the *lune*, factored with the inner products $-(\hat{\mathbf{R}} \cdot \hat{\mathbf{u}})$ and $(\hat{\mathbf{u}} \cdot \hat{\mathbf{o}})$ which is the part of the starlight that is directed towards the observer and with $|\mathbf{R}|^{-2}$, the inverse square relation between the light intensity and distance. De factor $\frac{4}{\pi}$ is to normalize the light-curve so that the value for a spherical mirror is equal to 1 for all possible $\hat{\mathbf{o}}$. This is illustrated in figure 6.

Figure 6: An ellipsoid orbiting a star with the light-rays of the starlight following the vectors $\mathbf{R}$ and $\mathbf{o}$. At each infinitesimal surface area $d^2\mathbf{s}$, we calculate the starlight that gets reflected in the direction of the observer under the assumption of Lambertian reflection.

This integral over $\mathbf{s}$ is difficult to calculate due to the properties of the surface of ellipsoids. That is why we want to rewrite this to an integral over $\hat{\mathbf{u}}$, so we can integrate over an unit sphere, which is far easier. We do this with the results of Appendix B, which in turn uses the result of Appendix A, which states that an element of the surface is given by

$$d^2\mathbf{s} = \frac{d^2\hat{\mathbf{u}}}{\kappa_1\kappa_2} = \frac{d^2\hat{\mathbf{u}}}{|A|\left(\hat{\mathbf{u}}^T A^{-1}\hat{\mathbf{u}}\right)^2},$$

where $|A|$ is the determinant of A and κ_1 and κ_2 are the principle curvature constants at $\mathbf{s}(\hat{\mathbf{u}})$. The Gaussian curvature K, the product of the two principal curvature constants in Cartesian coordinates is equal to [24]:

$$K = \kappa_1\kappa_2 = \frac{h^4}{a^2b^2c^2} = \frac{1}{a^2b^2c^2}\left(\frac{x^2}{a^4} + \frac{y^2}{b^4} + \frac{z^2}{c^4}\right)^{-2}.$$

In $\hat{\mathbf{u}}$ coordinates, this becomes:

$$K = |A|(\mathbf{s}^T A^2 \mathbf{s})^{-2} = |A||A\mathbf{s}|^{-4} = |A|u^{-4} = |A|\left|A^{-1/2}\hat{\mathbf{u}}\right|^4.$$

where $h = \left|A^{-1/2}\hat{\mathbf{u}}\right|$ is the distance between the surface point and the center of the ellipsoid. In the special case when we look at the surface of a sphere, where $a = b = c = r$ and $\hat{\mathbf{u}} = \hat{\mathbf{r}}$, where r is the radius and $\mathbf{r}$ the surface vectors, then $\left|A^{-1/2}\hat{\mathbf{u}}\right| = |r\hat{\mathbf{r}}| = r$.
Now we see that we rewrite the result of Appendix B to

$$d^2\mathbf{s} = \frac{d^2\hat{\mathbf{u}}}{|A||A^{-1/2}\hat{\mathbf{u}}|^4},$$

where

$$A^{-1/2} = \begin{pmatrix} a & 0 & 0 \\ 0 & b & 0 \\ 0 & 0 & c \end{pmatrix}$$

in the co-rotating frame.

With this result, we can rewrite equation 3 into,

$$f(t) = \frac{4}{\pi|A|} \int \int_{\mathbb{D}} \frac{\mathrm{d}^2\hat{\mathbf{u}}}{|\mathbf{R}|^2 \, |A^{-1/2}\hat{\mathbf{u}}|^4} \left(-\hat{\mathbf{R}}^T \hat{\mathbf{u}}\hat{\mathbf{u}}^T \hat{\mathbf{o}} \right). \tag{4}$$

Under our assumptions, $R = |\mathbf{R}|$ does not depend on $\mathbb{D}$, so that we can simplify equation 4 further into

$$f(t) = \frac{4}{\pi|A|R^2} \int \int_{\mathbb{D}} \frac{\mathrm{d}^2\hat{\mathbf{u}}}{|A^{-1/2}\hat{\mathbf{u}}|^4} \left(-\hat{\mathbf{R}}^T \hat{\mathbf{u}}\hat{\mathbf{u}}^T \hat{\mathbf{o}} \right). \tag{5}$$

2.3. Fourier series

As light-curves are periodic under our assumptions, we can express the light-curve as a Fourier series. One can use the Fourier coefficients in order to determine the dimensions and the orientation of a planet. A benefit of determining the dimensions and orientations with the Fourier coefficients and not with the light-curve directly, is that in this way, one can use this to filter noise of frequencies other than those that determine the calculated light-curve. Examples are the radio waves of pulsars and the orbital period of the star, given that those frequencies are not multiples of those frequencies that determine the calculated light-curve. Also, as light-curves are two dimensional graphs, it is easier to determine properties of light-curves with Fourier coefficients, which are numbers.

We will denote the Fourier coefficients by a_i with $i \in \{\mathbb{N} \cup \{0\}\}$ and b_j with $j \in \mathbb{N}$ so that

$$f(t) = a_0 + \sum_{n=1}^{\infty} a_n \cos(n\omega t) + b_n \sin(n\omega t). \tag{6}$$

The light-intensity of the planet is given by the light-curve multiplied with the light-intensity of its parent star. Note that we already took the distance to its parent star into account when we derived the light-curve. Because the light-intensity of stars are not constant due to intrinsic stellar variability, we can generally not observe Fourier coefficients below $10^{-3}a_0$ [25].

3.   Solar system triaxially-shaped dwarf planet

3.1.   Rapid spinning triaxially-shaped dwarf planet at superior conjunction

We now will apply equation 5 for the light-curve of a dwarf planet, located at superior conjunction in our solar system. Our goal is to determine the Fourier coefficients corresponding to the light-curve.
At conjunction, the Earth and the planet in question are aligned with the sun so that $\hat{\mathbf{o}} = -\hat{\mathbf{R}} = \mathbf{i}$

$$\hat{\mathbf{o}} = \begin{pmatrix} 1 \\ 0 \\ 0 \end{pmatrix}.$$

We assume that the rotational period of the planet is short enough and the orbital radius of the planet is long enough so that $\hat{\mathbf{o}}$ does not significantly change within one rotation of the planet. Then we can take $\hat{\mathbf{o}}$ constant. An example for a planet that fits the requirements for this application is the plutoid Haumea. Haumea has a rotational period of only 3.9 hours and lies between 35 and 52 times farther from the sun than Earth [5]. The triaxial shape of Haumea along with its rapid spinning is thought to be caused by a collision, rather than by gravitational effects [16]. The shape of Haumea is shown in an artist's conception of Haumea in figure 7.
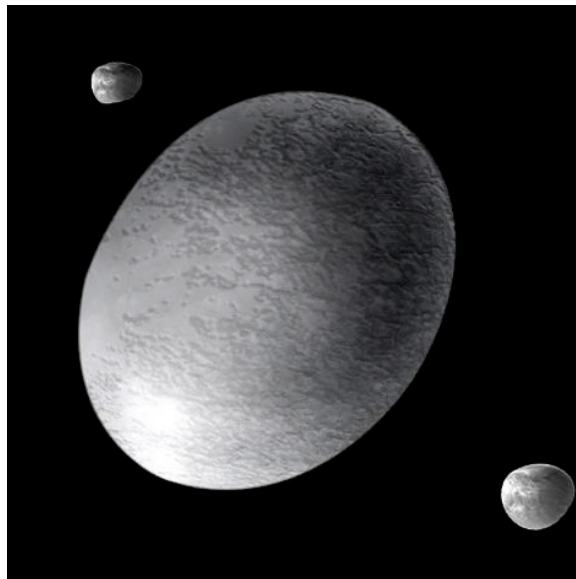
Figure 7: An artist's conception of Haumea with its moons Hi'iaka and Namaka [16]. Here the triaxial shape of Haumea is shown.

To calculate the light-curve of equation 5, we rewrote the integral over the surface of the planet to an integral over an unit sphere. Therefore, we take $\hat{\mathbf{u}}$ in spherical coordinates

$$\hat{\mathbf{u}} = \begin{pmatrix} \cos\phi\sin\theta \\ \sin\phi\sin\theta \\ \cos\theta \end{pmatrix},$$

with the polar angle θ and azimuthal angle ϕ. Because the planet is rotating, we substitute ϕ with $\phi + \Omega t$, where Ω is the rotational angular frequency of the planet. In order to calculate the light-curve given by equation 5, we need to calculate

$$|A| = (abc)^{-2}, \quad \left|A^{-1/2}\hat{\mathbf{u}}\right|^2 = (a^2\cos^2\phi + b^2\sin^2\phi)\sin^2\theta + c^2\cos^2\theta \quad \text{and} \quad \mathrm{d}^2\hat{\mathbf{u}} = \sin\theta\mathrm{d}\theta\mathrm{d}\phi.$$

13

and we need to evaluate the inner products

$$\hat{\mathbf{u}} \cdot \hat{\mathbf{o}} = \cos(\phi + \Omega t) \sin \theta \quad \text{and} \quad -\hat{\mathbf{R}} \cdot \hat{\mathbf{u}} = \cos(\phi + \Omega t) \sin \theta$$

With this, equation 5 becomes :

$$f(t) = \frac{4}{\pi} \left(\frac{abc}{R} \right)^2 \int \int_{\mathbb{D}} \sin^3 \theta \left(\frac{\cos(\phi + \Omega t)}{(a^2 \cos^2 \phi + b^2 \sin^2 \phi) \sin^2 \theta + c^2 \cos^2 \theta} \right)^2 \mathrm{d}\phi \mathrm{d}\theta.$$

By writing $\cos(\phi + \Omega t)$ as $(e^{\phi + \Omega t} + e^{-(\phi + \Omega t)})/2$, we see that can rewrite the integrand as follows:

$$c_1 + c_2(e^{-2i\Omega t} + e^{2i\Omega t}) = c_1 + 2c_2 \cos 2\Omega t,$$

where c_1 and c_2 are real constants. As we do not have to integrate over t, the light-curve can also be written as follows

$$f(t) = a_0 + \frac{a_2}{2} \left(e^{-2i\Omega t} + e^{2i\Omega t} \right) = a_0 + a_2 \cos(2\Omega t),$$

where a_0 and a_2 are real constants for the planet. That means that a_0 and a_2 are the only non-zero Fourier coefficients of the light-curve. This could have been expected because the mean of the light-curve, a_0, is greater than zero as the observer always receives some light from a planet at superior conjunction and light-intensity is always positive. Also, because a triaxial is symmetric in its three mirror planes, we expect that there the frequency of the light-curve is twice that of the frequency of its rotation around its own spin axis, hence a non-zero a_2.

At conjunction, as the orbit of the outer solar system objects is far greater than that of earth, we always observe them at full phase, so that ϕ and θ must both be integrated over $[0, \pi]$. That is, the *lune* $\mathbb{D} = \{(\phi, \theta) : 0 \leq \theta \leq \pi, 0 \leq \phi \leq \pi\}$. We can analytically simplify the expressions for these constants by executing the integral over ϕ. The constants a_0 and a_2 are then given by [6]

$$a_0 = 4 \left(\frac{abc}{R} \right)^2 \int_0^\pi \frac{((a^2 + b^2) \sin^2 \theta + 2c^2 \cos^2 \theta) \sin^3 \theta}{(a^2 \sin^2 \theta + c^2 \cos^2 \theta)^{3/2} (b^2 \sin^2 \theta + c^2 \cos^2 \theta)^{3/2}} \mathrm{d}\theta$$

and [6]

$$a_2 = 2 \left(\frac{abc}{R} \right)^2 (b^2 - a^2) \int_0^\pi \frac{\sin^5 \theta}{(a^2 \sin^2 \theta + c^2 \cos^2 \theta)^{3/2} (b^2 \sin^2 \theta + c^2 \cos^2 \theta)^{3/2}} \mathrm{d}\theta.$$
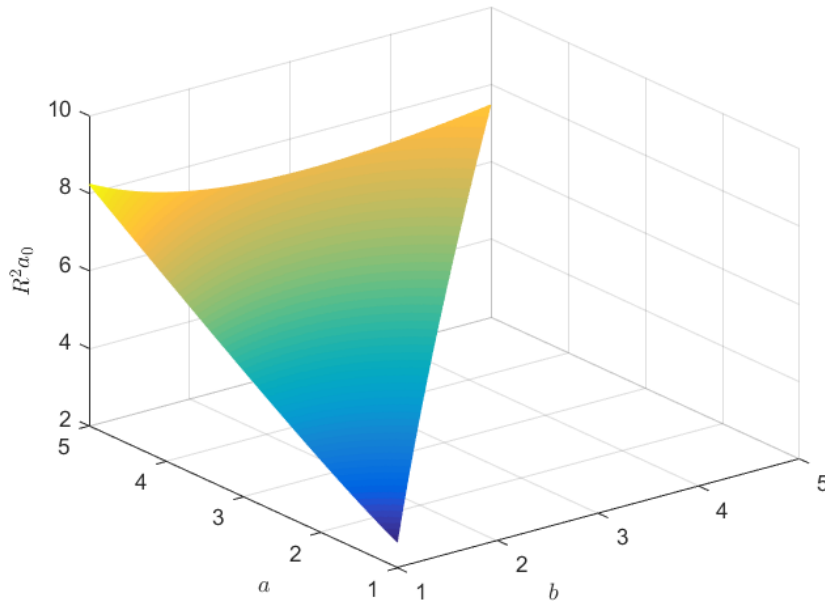
Figure 8: The coefficient $R^2 a_0$ for $\{(a, b)|5 \geq a \geq b \geq c = 1\}$.
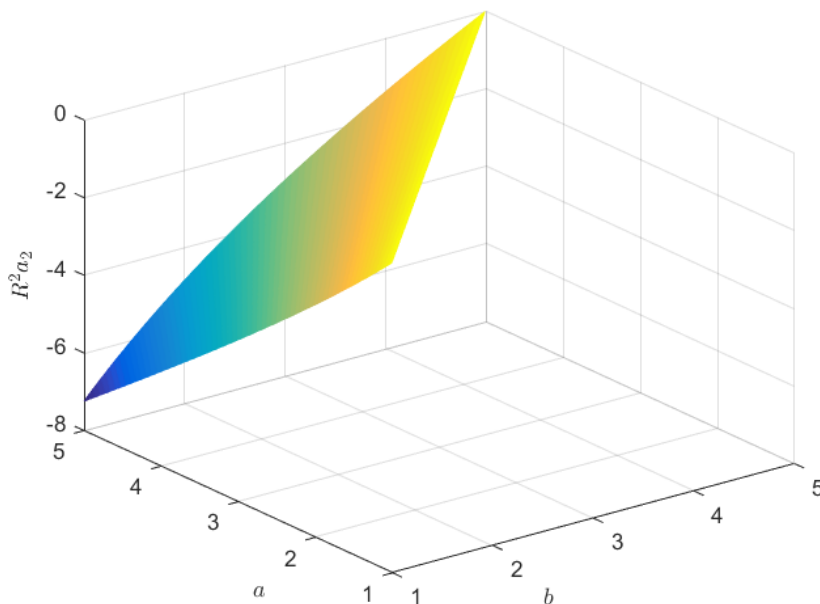
Figure 9: The coefficient $R^2 a_2$ for $\{(a,b)|5 \geq a \geq b \geq c = 1\}$.

Figures 8 and 9 respectively show the numerically determined values for $R^2 a_0$ and $R^2 a_2$ for $\{(a,b)|5 \geq a \geq b \geq c = 1\}$. First of all, we notice that a_2 is strictly negative for triaxially-shaped planets. We do see that a_2 is zero for $a = b$, but those planets are spheroidally-shaped, not triaxially-shaped. a_2 is zero for spheroidally shaped planets, as those planets are symmetrical around their rotation axes. Therefore a spheroidally shaped planet gives a constant light-curve, as a_0 is strictly positive.

Due to the orientation of the planet in respect to the observer at $t = 0$, the light-curve starts at a minimum. Because $\cos(2\Omega t)$ decreases for increasing $0 \leq \Omega t \leq \pi/2$ and the light-curve starts at a minimum, it is logical that a_2 is strictly negative for triaxally-shaped planets.

Secondly, we notice that a_2 has its minimum at $a = 5$ and $b = 1$. This is because the difference between the maximum and the minimum of the light-curve is the largest the greater the difference between a and b is.

Thirdly, we notice that for constant a, a_0 does not necessarily increase with increasing b. The planet does become larger for increasing b, so that the total area from which the observer receives light increases. But the planet also becomes less flat so that the percentage of reflected light that the observer receives decreases. At first when increasing b from 1, the percentage of light that is reflected towards the observer decreases more than the area of the planet increases, resulting into smaller values for a_0. But later, the area of the planet increases more than the percentage of light that is reflected towards the observer decreases, resulting into greater values for a_0.

3.2.   Haumea

Now we will look at our example of a rapid spinning triaxial planet at superior conjunction, Haumea. The approximate ratio of the lengths of the semi-principle axes of Haumea is given by $a : b : c = 1.94 : 1.56 : 1$ [5]. In [5], they assumed Haumea is a Jacobi ellipsoid and with a mesh of 4000 triangular facets and the Hapke photometric model, they calculated the light-curve for a range of possible lengths of the semi-principal axes until they found a match with the measurements. Our calculations from the previous section give the light-curve as shown in figure 10.
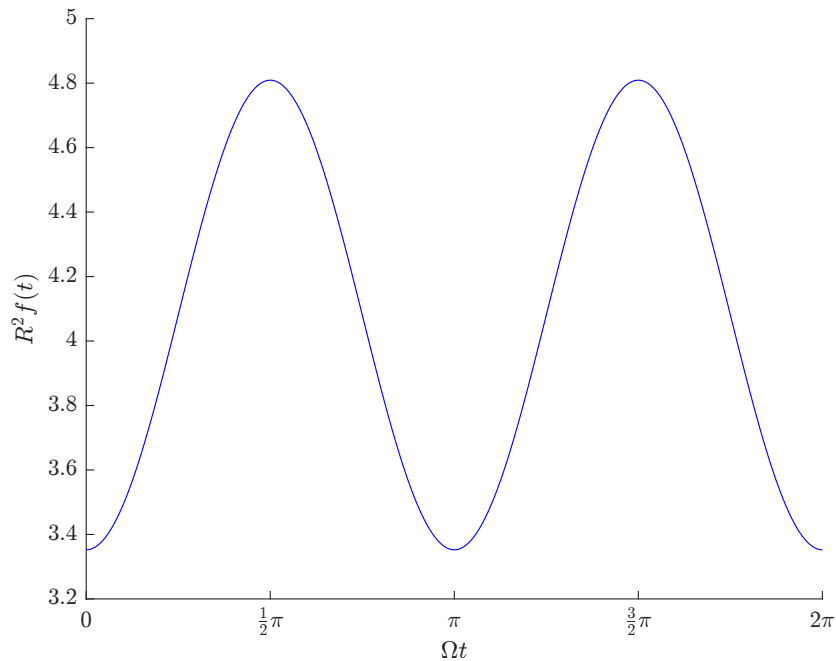
Figure 10: The light-curve for the plutoid Haumea for $a : b : c = 1.94 : 1.56 : 1$ [5].

Now we are going to compare this result with measurement data given in figure 11 [5].
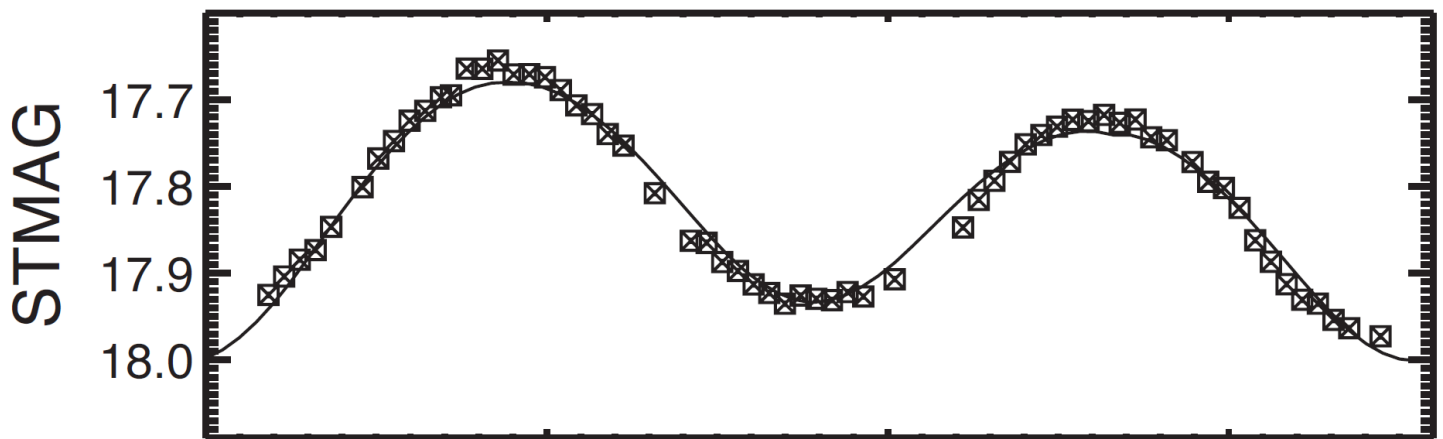
Figure 11: Measurement data of Haumea on 2009 February using the PC chip on the Wide Field/Planetary Camera 2 on Hubble space telescope. The data is given in magnitudes over a single rotational period. The fit is that of a Jacobi ellipsoid. [5]

We notice that as with our model, we see 2 periods in one rotational period of the measured light-curve. However, the second period has a smaller difference between its minimum and maximum, which could be explained by a darker and lighter side of Haumea. We also notice that the fit in figure 11 does take the alternating difference between the minimum and maximum of the light-curve into account. This can be explained as we assume Lambertian reflection and the Hapke photometric model does not. Therefore, the Hapke model may give a non-zero a_4. Haumea is thus not a perfect homogeneous Lambertian reflector.
If we look at the difference between the maxima and the minima of the calculated light-curve and the data, we see that the calculated light-curve has a difference of 0.4 magnitudes compared to the difference of 0.32 magnitudes given by the measured light-curve. Note that we could use the light-curve given by figure 10 here as the relative difference does not change when we scale the light-curve to compare the calculated

light-curve with the data.

Now to compare the mean values of the calculated light-curve and the data, we need to convert our model to apparent magnitudes. First we calculate the light-intensity which an observer would receive. This is given by

$$\frac{1}{4\pi|\mathbf{o}|^2}f(t),$$

where $|\mathbf{o}|$ is the distance between the observer and Haumea. The light-curve given by figure 10 is for the ratio between the lengths of the semi-principle axes for $c = 1$. Therefore we have to multiply it by the square of 495km [5], half the actual size of the shortest semi-principle axis.

Due to our normalization of the light-curve, we have to divide the light-curve by 4 to get an apparent magnitude of 0 for the Sun, while the Sun has an apparent magnitude -26.74 [19]. To convert our model to apparent magnitudes, we need to add our value for the light-intensity the observer receives multiplied with $4\pi(1AU)^2$, to the apparent magnitude of the Sun. With $R = 50.64AU$, $|o| = 50.63AU$ [14] and the mean value of $R^2 f(t)$ of 4, the apparent magnitude of Haumea is then given by

$$-26.74 - 5 \cdot [\log_{10}(495\text{km}) + \log_{10}(1\text{AU}) - \log_{10}(50.63\text{AU}) - \log_{10}(50.64\text{AU})] = 17.70.$$

The mean of the data given in figure 11 is given by the apparent magnitude of 17.84. This 0.14 magnitude difference could be explained by an average albedo of 0.88 in line with [26].

Besides confirming the dimensions of Haumea, we also want to determine the values of a, b and c from the data. As aforementioned, we can not determine the values of a, b and c from only two non-zero real Fourier coefficients. In figure 5 we show a diagram that relate b/a to c/a for Jacobi ellipsoids. With that relation and a_0 and a_2, we can determine the values of a, b and c.

Note that the values of a_2 and a_0 as shown in figures 8 and 9 should be multiplied with c^2 to compare them to the measurements. However, a_2/a_0 can be directly compared to the measurement results. In figure 12 we show the numerically determined values of a_2/a_0 for $\{(a,b)|5 \geq a \geq b \geq c = 1\}$.
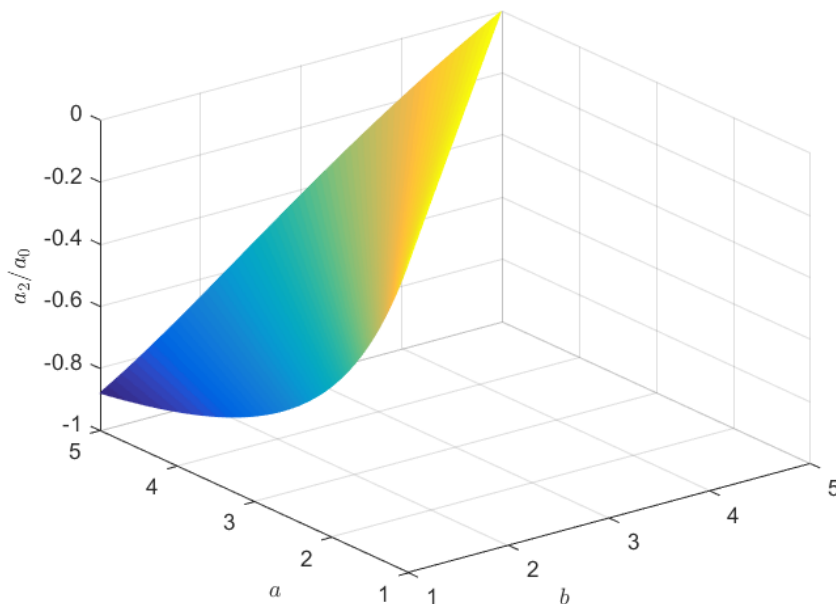
Figure 12: a_2/a_0 for $\{(a,b)|5 \geq a \geq b \geq c = 1\}$.

As aforementioned, the difference between the maximum and minimum value of the measured light-curve of Haumea is 0.32 magnitude. As this difference is $2a_2$, we conclude that $a_2 = 0.08a_0$. With figure 12, we now get a curve for possible values of a and b that we can compare to the curve given by [15]. We find that within reading errors, the ratio given by [5] is feasible. With this ratio, we can calculate the value of R^2a_0 of figure 8 and calculate the value of c if the albedo is known.

4.   Spheroidally-shaped exoplanet

The second application we consider is a spheroidally-shaped exoplanet. This is a flattened sphere for which the semi-principle axis are $a = b > c$. An example of a spheroid is the planet Saturn. The approximate ratio for the semi-principle axes $a : b : c$ of Saturn is $1 : 1 : 0.935$ [27]. The spheroidal shape of Saturn is shown in figure 13.
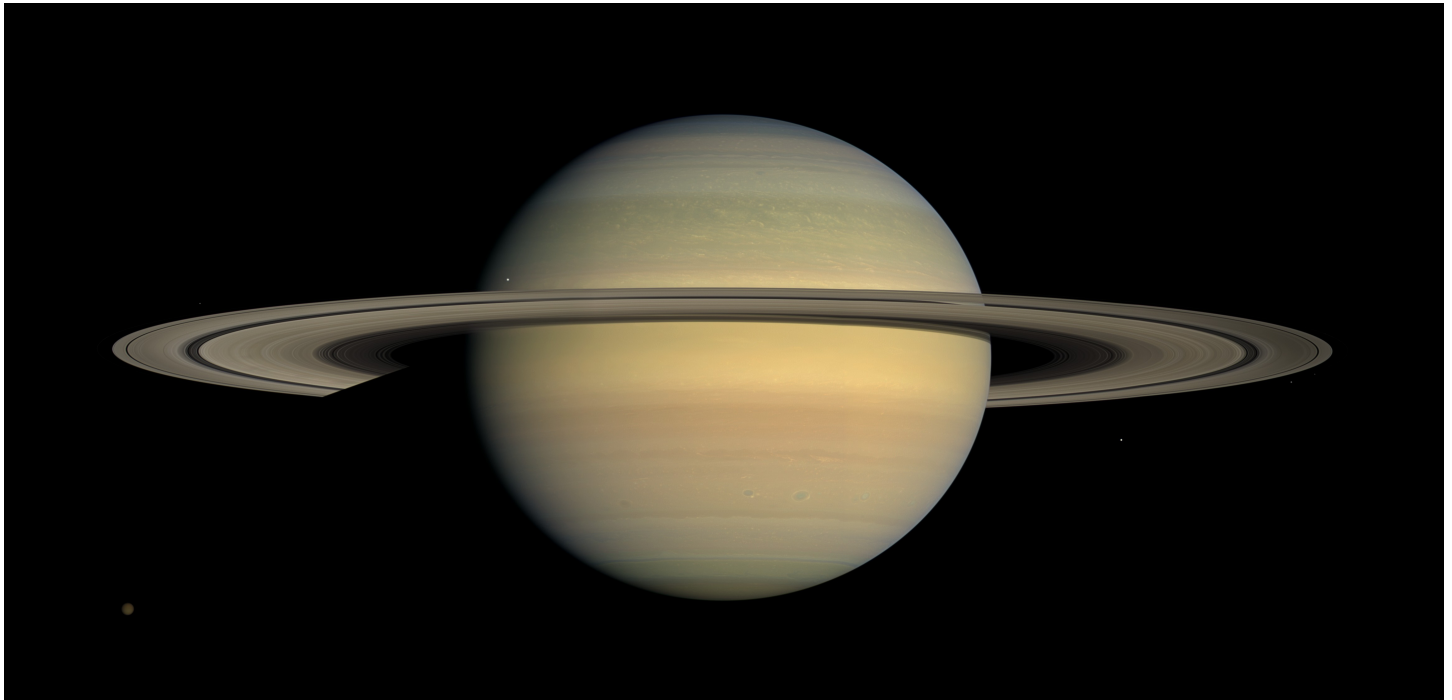
Figure 13: An image photographed by Cassini in July 2008 of Saturn approaching equinox [28]. Here the spheroidal shape of Saturn is shown.

With our assumption that the planet is homogeneous, the spin of the planet around its spin axis $\mathbf{c}$ does not affect the light-curve. This is because a spheroidally-shaped planet is symmetrical around its spin axis. Therefore, we do not consider the light-curve of the planet throughout a rotation around its own axis, but throughout an orbit around its parent star. As the spin of the planet does not affect the light-curve, we can assume that the planet does not spin.

We will consider two possible orientations for the observer to view the exoplanetary system in respect to the orbital plane. The orbital plane is defined by $\mathbf{i}$ and $\mathbf{j}$ with the normal $\mathbf{k}$. We will consider the case with the observer positioned in the orbital plane. We denote this case as edge-on observation. We will also consider the case with the observer positioned perpendicular to the orbital plane. We denote this case as face-on observation.

Moreover, we also consider all possible orientations the planet can have. We denote the case with the semi-principle axes $\mathbf{a}, \mathbf{b}$ and $\mathbf{c}$ respectively aligned with the basis $\mathbf{i}, \mathbf{j}$ and $\mathbf{k}$ when $\hat{\mathbf{R}} = \mathbf{i}$ as zero tilt.

In section 4.1 we will first consider the case without tilt at edge-on observation. Then in section 4.2 we will consider the case without tilt at face-on observation. Thirdly in section 4.3 we will consider the case with non-zero tilt at edge-on observation. Lastly in section 4.4 we will consider the case with non-zero tilt at face-on observation.

4.1.   Spheroidally-shaped exoplanet without tilt at edge-on observation

In figure 14, we show a spheroidally-shaped planet without tilt in four different locations in its orbit around its parent star. Notice that **a** and **b** are in the orbital plane as the planet has no tilt. Also notice that the spin axis **c** and the orbit axis **k** are parallel.
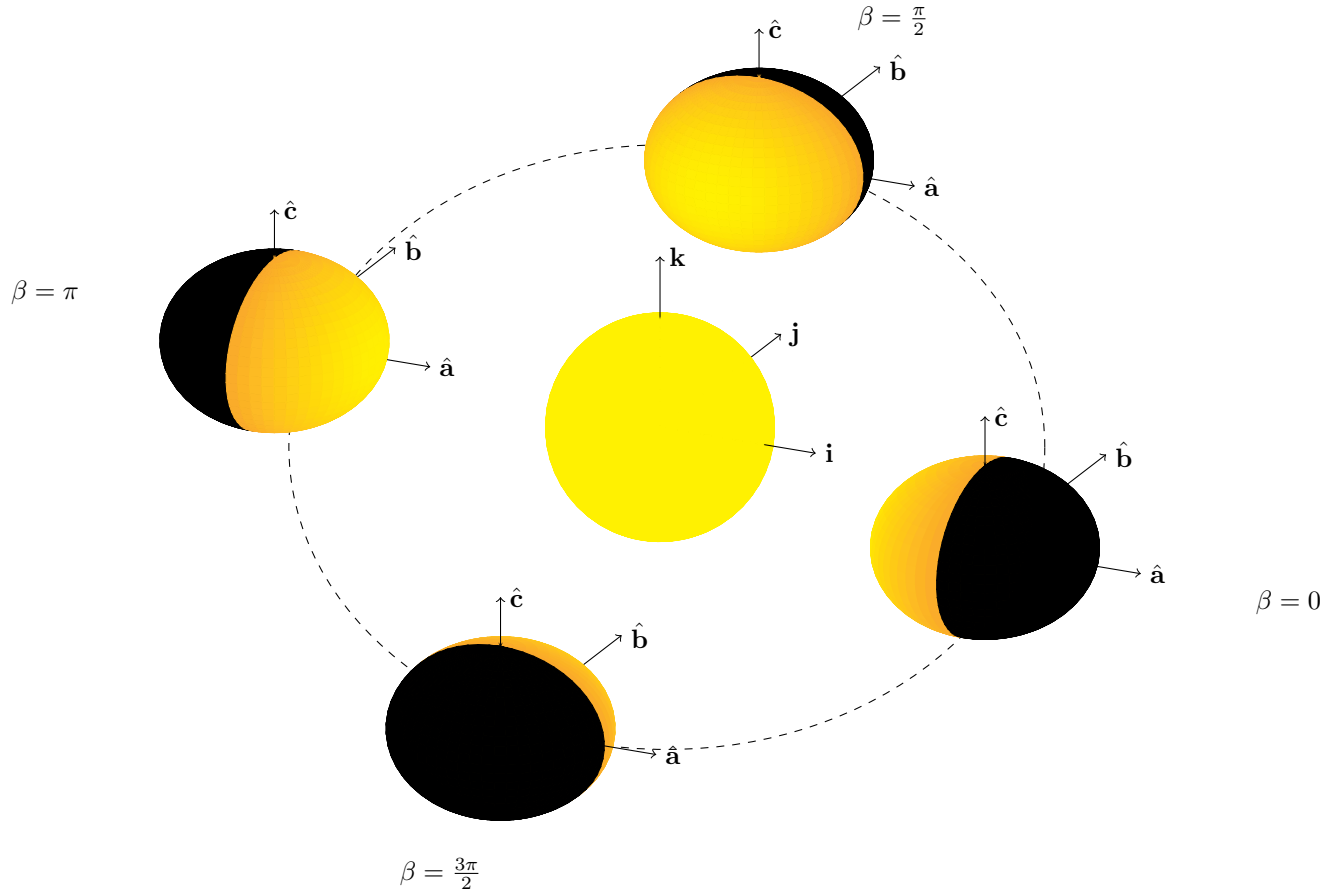
Figure 14: A spheroidally-shaped planet with zero tilt in four different locations in an orbit around its parent star. Notice that **a** and **b** are in the orbital plane as the planet has no tilt. Also notice that the spin axis **c** and the orbit axis **k** are parallel.

For the case without tilt at edge-on observation, we expect that the light-curve of a spheroidally-shaped planet and the light-curve of a spherical exoplanet only differ by a constant. We expect this as for edge-on observation without tilt, a spheroid has the same rotational symmetries as a sphere. After all, a sphere is a special case of a spheroid.

As in the case of a solar system triaxially-shaped dwarf planet, we take $\hat{\mathbf{u}}$ in spherical coordinates

$$\hat{\mathbf{u}} = \begin{pmatrix} \cos\phi\sin\theta \\ \sin\phi\sin\theta \\ \cos\theta \end{pmatrix}.$$

In contrast to the case of a solar system triaxially-shaped dwarf planet though, $\hat{\mathbf{u}}$ is time-independent as

we can assume that the planet does not spin. As we consider the case of edge-on observation we take

$$\hat{\mathbf{o}} = \mathbf{i} = \begin{pmatrix} 1 \\ 0 \\ 0 \end{pmatrix}.$$

Under our assumption of a circular orbit, we take

$$\hat{\mathbf{R}} = \begin{pmatrix} \cos\beta \\ \sin\beta \\ 0 \end{pmatrix},$$

where β is the orbital phase dependent on time. β is congruent with $\omega t \bmod 2\pi$. Here ω is the rotational angular frequency and t time. $\hat{\mathbf{R}}$ is chosen so that for $\beta = 0$, $\hat{\mathbf{R}} = \hat{\mathbf{o}}$. In order to calculate the light-curve given by equation 5, we calculate the inner products

$$-\hat{\mathbf{R}} \cdot \hat{\mathbf{u}} = -\sin\theta\cos(\beta - \phi) \quad \text{and} \quad \hat{\mathbf{u}} \cdot \hat{\mathbf{o}} = \cos\phi\sin\theta.$$

We also calculate the other components of equation 5 for $a = b$

$$|A| = a^{-4}c^{-2}, \quad \left|A^{-1/2}\hat{\mathbf{u}}\right|^2 = a^2\sin^2\theta + c^2\cos^2\theta \quad \text{and} \quad \mathrm{d}^2\hat{\mathbf{u}} = \sin^2\theta\,\mathrm{d}\phi\,\mathrm{d}\theta.$$

Now we have to determine the integration domain. Therefore, we calculate the terminator, the boundary between the illuminated and unilluminated side of the planet. Due to our approximation that the light from the parent star follows $\hat{\mathbf{R}}$, the terminator is given by $-\hat{\mathbf{R}} \cdot \hat{\mathbf{u}} = 0$

$$\hat{\mathbf{R}} \cdot \hat{\mathbf{u}} = 0 \quad \text{for} \quad \theta = 0 \vee \theta = \pi \vee \phi = \beta + n\pi, \text{ with } n \in \mathbb{Z}.$$

We also calculate the limb, the boundary between the side of the planet the observer can and cannot see. The limb is given by $\hat{\mathbf{u}} \cdot \hat{\mathbf{o}} = 0$, due to the same approximation as with the terminator that the light from the parent star follows $\hat{\mathbf{R}}$

$$\hat{\mathbf{u}} \cdot \hat{\mathbf{o}} = 0 \quad \text{for} \quad \theta = 0 \vee \theta = \pi \vee \phi = \pi/2 \vee \phi = 3\pi/2$$

Now we have calculated the terminator and the limb, we calculate that the integration domain is given by $\mathbb{D} = \{(\phi, \theta) : 0 \le \theta \le \pi, \phi \in \Phi\}$, with

$$\Phi = \begin{cases} [3\pi/2, 3\pi/2 + \beta] & 0 \le \beta < \pi \\ [-3\pi/2 + \beta, \pi/2] & \pi \le \beta < 2\pi \end{cases}.$$

Now we calculate the light-curve of equation 5

$$\begin{aligned}
f(t) &= -\frac{4a^4c^2}{\pi R^2} \int_0^\pi \frac{\sin^3\theta}{[a^2\sin^2\theta + c^2\cos^2\theta]^2}\mathrm{d}\theta \int_\Phi \cos\phi\cos(\beta - \phi)\mathrm{d}\phi \\
&= -\frac{a^4c^2}{\pi R^2} \int_0^\pi \frac{\sin^3\theta}{[a^2\sin^2\theta + c^2\cos^2\theta]^2}\mathrm{d}\theta[2\phi\cos\beta - \sin(\beta - 2\phi)]_\Phi \\
&= -\frac{2a^4c^2}{\pi R^2} \int_0^\pi \frac{\sin^3\theta}{[a^2\sin^2\theta + c^2\cos^2\theta]^2}\mathrm{d}\theta \begin{cases} \beta\cos\beta - \sin\beta & 0 \le \beta \le \pi \\ (2\pi - \beta)\cos\beta + \sin\beta & \pi \le \beta \le 2\pi \end{cases}.
\end{aligned} \quad (7)$$

Here we could separate the variables ϕ and θ since the denominator of the integrand of the light-curve became independent of ϕ as a is equal to b. Notice that the integral over θ is a prefactor independent

of β. Also notice that the part of the light-curve that depends on β does not depend on a and c. This means that, as expected, without tilt at edge-on observation, the light-curve of exoplanets with different ellipsoidal shape only differ by a constant. The consequence of this is that for edge-on observation, we can for example not differentiate between a sphere and a general spheroid. The light-curve of a spheroid without tilt at edge-on observation is affected both by the shape and the overall size of the planet in the same manner. Thus without knowing the size of the planet, we cannot determine the shape of the planet.

In figure 15 we show the light-curve given by equation 7 for several values of the ratio between a and c.
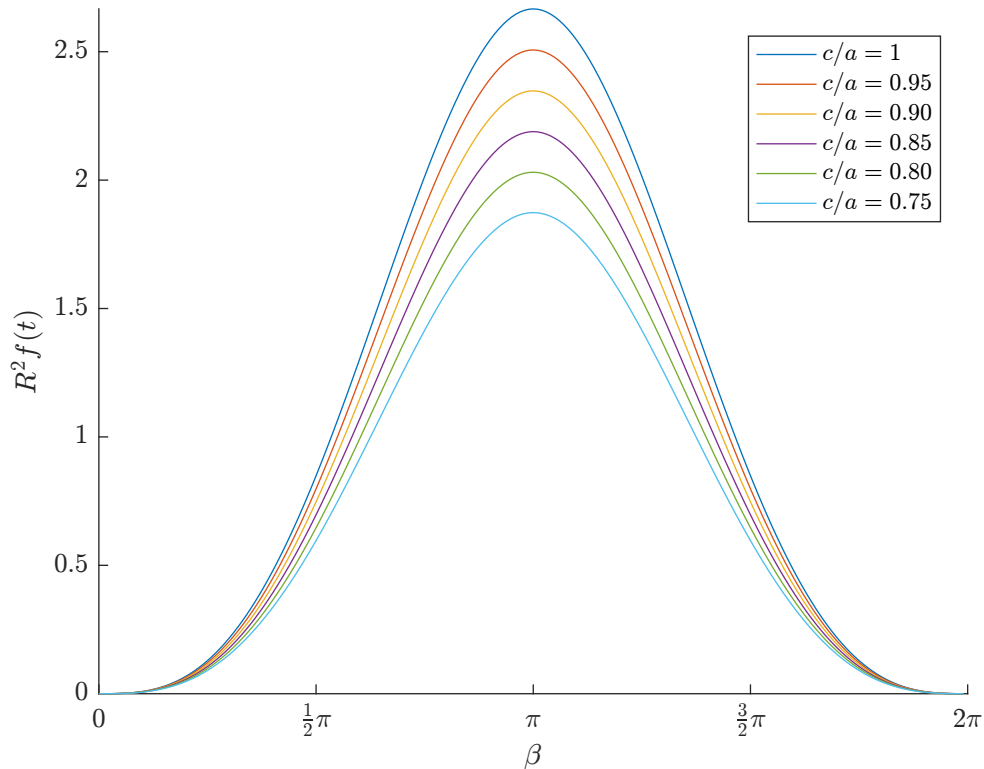
Figure 15: $R^2 f(t)$ against β for spheroidally-shaped exoplanets for several values of c/a at edge-on observation. The top light-curve, with the $c/a = 1$, is a sphere.

We notice a few characteristics of the light-curve in figure 15. Firstly, we notice that the maximum of all the light-curves are at $\beta = \pi$. This can be expected as the integration domain for $\beta = \pi$ is the largest and the integral is always positive.
Secondly we notice that the light-curves are also symmetrical around $\beta = \pi$. This can be explained due to the fact that a spheroidally-shaped planet without tilt is symmetric around its spin axis and the orbit of the planet is symmetric around the orbit axis.
Furthermore, we notice that the light-curves are consistently lower for smaller values of c/a. This can be explained as the planet becomes physically smaller for smaller values of c/a for fixed a. The effect we saw in the case of a solar system triaxially-shaped dwarf planet, that even though the planet reflects less light as it is smaller as a greater percentage of the light is reflected towards the observer is not present here. This is because we adjust the **c**-axis which is perpendicular to $\hat{\mathbf{o}}$.

4.2.   Spheroidally-shaped exoplanet without tilt at face-on observation

Now we consider the case of a spheroidally-shaped exoplanet without tilt at face-on observation. In this case, we expect the light-curve to be a constant. Note that $\hat{\mathbf{o}}$ is parallel to the orbit axis around which the orbit of the planet is symmetric

$$\hat{\mathbf{o}} = \mathbf{k} = \begin{pmatrix} 0 \\ 0 \\ 1 \end{pmatrix}.$$

This symmetry, the assumption that the planet is homogeneous and the fact that spin does not affect the light-curve in this situation, make us suspect a light-curve that is flat.
To calculate the light-curve given by equation 5 for this case, we use the same method as with the edge-on case.

The change of $\hat{\mathbf{o}}$ only changes $\hat{\mathbf{u}} \cdot \hat{\mathbf{o}}$ in respect to the case of edge-on observation

$$\hat{\mathbf{u}} \cdot \hat{\mathbf{o}} = \cos\theta.$$

Due to the change of $\hat{\mathbf{u}} \cdot \hat{\mathbf{o}}$, the limb also changes in respect to the case of edge-on observation

$$\hat{\mathbf{u}} \cdot \hat{\mathbf{o}} = 0 \quad \text{for} \quad \theta = \pi/2 \vee \theta = 3\pi/2.$$

If we calculate the integration domain, we get $\mathbb{D} = \{(\phi, \theta) : 0 \leq \theta \leq \pi/2, \phi \in \Phi\}$, with

$$\Phi = [\pi/2 + \beta, 3\pi/2 + \beta].$$

As all the other components of the light-curve given by equation 5 are the same for the case of face-on observation as the case of edge-on observation, the light-curve is given by

$$\begin{aligned}
f(t) &= -\frac{4a^4c^2}{\pi R^2} \int_0^\pi \frac{\cos\theta\sin^2\theta}{[a^2\sin^2\theta + c^2\cos^2\theta]^2}\mathrm{d}\theta \int_\Phi \cos(\beta - \phi)\mathrm{d}\phi \\
&= \frac{4a^4c^2}{\pi R^2} \int_0^\pi \frac{\cos\theta\sin^2\theta}{[a^2\sin^2\theta + c^2\cos^2\theta]^2}\mathrm{d}\theta[\sin(\beta - \phi)]_\Phi \\
&= \frac{8a^4c^2}{\pi R^2} \int_0^\pi \frac{\cos\theta\sin^2\theta}{[a^2\sin^2\theta + c^2\cos^2\theta]^2}\mathrm{d}\theta
\end{aligned} \tag{8}$$

Here we could again separate the variables ϕ and θ since the denominator of the integrand of the light-curve became independent of ϕ as a is equal to b. Notice again that the integral over θ is a prefactor independent of β. Because of that, the reflected light-intensity given by equation 8 is constant as argued.
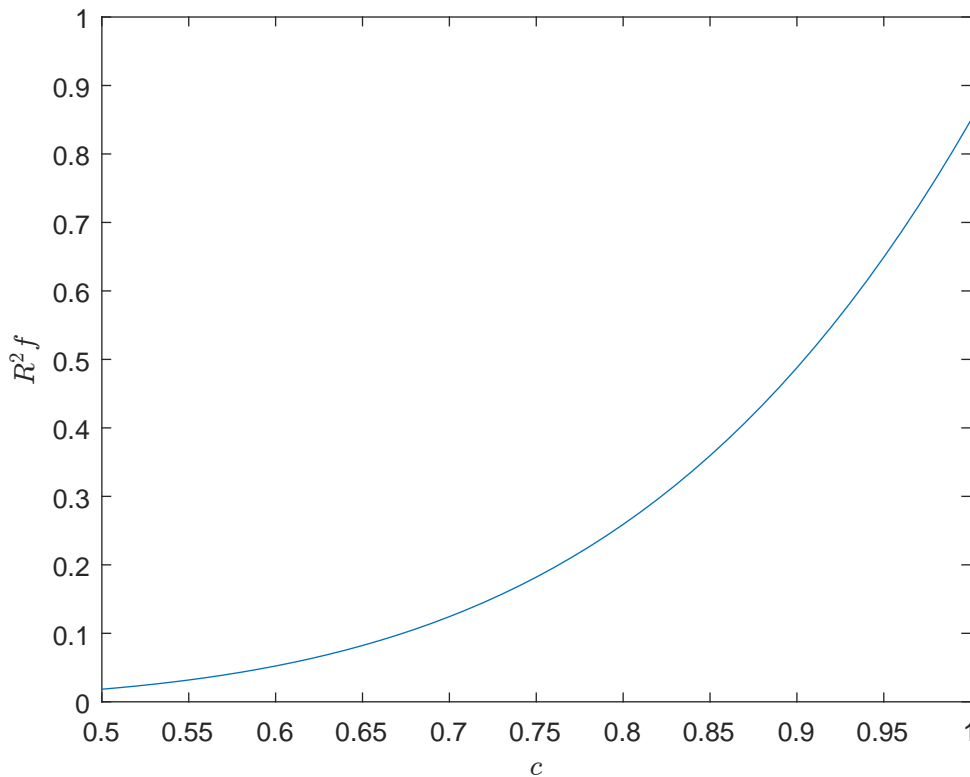
Figure 16: The reflected light-intensity of spheroidally-shaped exoplanets for $0.5 \leq c \leq 1$ with $a = b = 1$ without tilt at face-on observation.

The values of this flat light-curve are given in figure 16 for $0.5 \leq c \leq 1$ with $a = b = 1$. We notice that the light-curves converges to zero for smaller c. This is because the planet becomes flatter for smaller c and without tilt, the average normal of the reflective surface converges to $\mathbf{c}$ which is perpendicular to the incoming light.

4.3.   Spheroidally-shaped exoplanet with tilt at edge-on observation

Now we will consider a spheroidally-shaped exoplanet with tilt at edge-on observation. Examples of planets with tilt are Saturn with a tilt of 26.73° [28] and Earth with a tilt of 23.44° [20]. As all the information about the shape of the ellipsoid is contained in the matrix A, we can adjust A to take tilt into account without changing anything else of the light-curve given by equation 5. To adjust A, we use the rotation matrices

$$R_{\mathbf{j}}(\gamma) = \begin{pmatrix} \cos\gamma & 0 & \sin\gamma \\ 0 & 1 & 0 \\ -\sin\gamma & 0 & \cos\gamma \end{pmatrix} \quad \text{and} \quad R_{\mathbf{k}}(\delta) = \begin{pmatrix} \cos\delta & -\sin\delta & 0 \\ \sin\delta & \cos\delta & 0 \\ 0 & 0 & 1 \end{pmatrix} \tag{9}$$

around the $\mathbf{j}$-axis and $\mathbf{k}$-axis respectively. We first rotate the planet around the $\mathbf{j}$-axis and secondly around the $\mathbf{k}$-axis. By rotating the planet in this manner, the spin axis $\hat{\mathbf{n}}$ of the planet

$$\hat{\mathbf{n}} = \begin{pmatrix} \cos\delta \sin\gamma \\ \sin\delta \sin\gamma \\ \cos\gamma \end{pmatrix}$$

has spherical coordinates. Now to take tilt into account, we have to substitute A in equation 5 with $A_{jk} = R_{\mathbf{k}}(\delta) R_{\mathbf{j}}(\gamma) A R_{\mathbf{j}}(\gamma)^T R_{\mathbf{k}}(\delta)^T$. We have chosen the rotation matrices so that the orbit axis and the

spin axis are parallel for $\gamma = 0$ and $\delta = 0$. Note that $A_{jk} = A$ for $\gamma = 0$ and $\delta = 0$. This is in accordance with our definition of no tilt. Note that $|A|$, the determinant of A, does not depend on tilt. Indeed, $|A_{jk}| = |A|$ for every possible tilt.

With everything else the same as in the case without tilt at edge-on observation, the light-curve given by equation 5 with tilt at edge-on observation becomes

$$f(t) = -\frac{4(abc)^2}{\pi R^2} \int \int_{\mathbb{D}} \frac{\cos\phi \sin^3\theta \cos(\beta - \phi)}{\left| A_{jk}^{-1/2}\hat{\mathbf{u}} \right|^4} \mathrm{d}\phi \mathrm{d}\theta, \tag{10}$$

where the integration domain is $\mathbb{D} = \{(\phi, \theta) : 0 \leq \theta \leq \pi, \phi \in \Phi\}$, with

$$\Phi = \begin{cases} [3\pi/2, 3\pi/2 + \beta] & 0 \leq \beta < \pi \\ [-3\pi/2 + \beta, \pi/2] & \pi \leq \beta < 2\pi \end{cases}$$

is the same as without tilt.

Now we consider the symmetries of a spheroidally-shaped exoplanet at edge-on observation to figure out for which tilts the light-curves are indistinguishable from each other. Firstly, the light-curve for values of γ that are equidistant to $\gamma = 0$, $\gamma = \pi/2$, $\gamma = \pi$ and/or $\gamma = 3\pi/2$ are the same. This is because for a homogeneous planet, the planet surface is at the exact same spot for values $\gamma = \pi$ apart. Furthermore, due to the edge-on observation and the symmetry of the planet along the plane coplanar to $\mathbf{a}$ and $\mathbf{b}$, the light-curve is the same for values of γ equidistant to $\gamma = 0$ and $\gamma = \pi$. Also, because the symmetry of the planet along the plane coplanar to $\mathbf{a}$ and $\mathbf{c}$, the light-curve is the same for values of γ equidistant to $\gamma = \pi/2$ and $\gamma = 3\pi/2$.
Also, the light-curve is the same for values of δ that are π apart because of the symmetry of the planet along the plane coplanar to $\mathbf{a}$ and $\mathbf{b}$.

In figure 17 we show the light-curves for edge-on observation for tilts with $0 \leq \gamma \leq \pi/2$ and $0 \leq \delta < \pi$ for spheroidally-shaped exoplanets with $c/a = 1$ through $c/a = 0.75$. Due to the aforementioned symmetries, there are no other distinct light-curves for other values of γ and δ. Note that $\gamma = 0$ describes the situation without tilt, which can be found in figure 15.

(a) $\delta = 0$ and $\gamma = \pi/4$

(b) $\delta = 0$ and $\gamma = \pi/2$

(c) $\delta = \pi/4$ and $\gamma = \pi/4$

(d) $\delta = \pi/4$ and $\gamma = \pi/2$

(e) $\delta = \pi/2$ and $\gamma = \pi/4$

(f) $\delta = \pi/2$ and $\gamma = \pi/2$
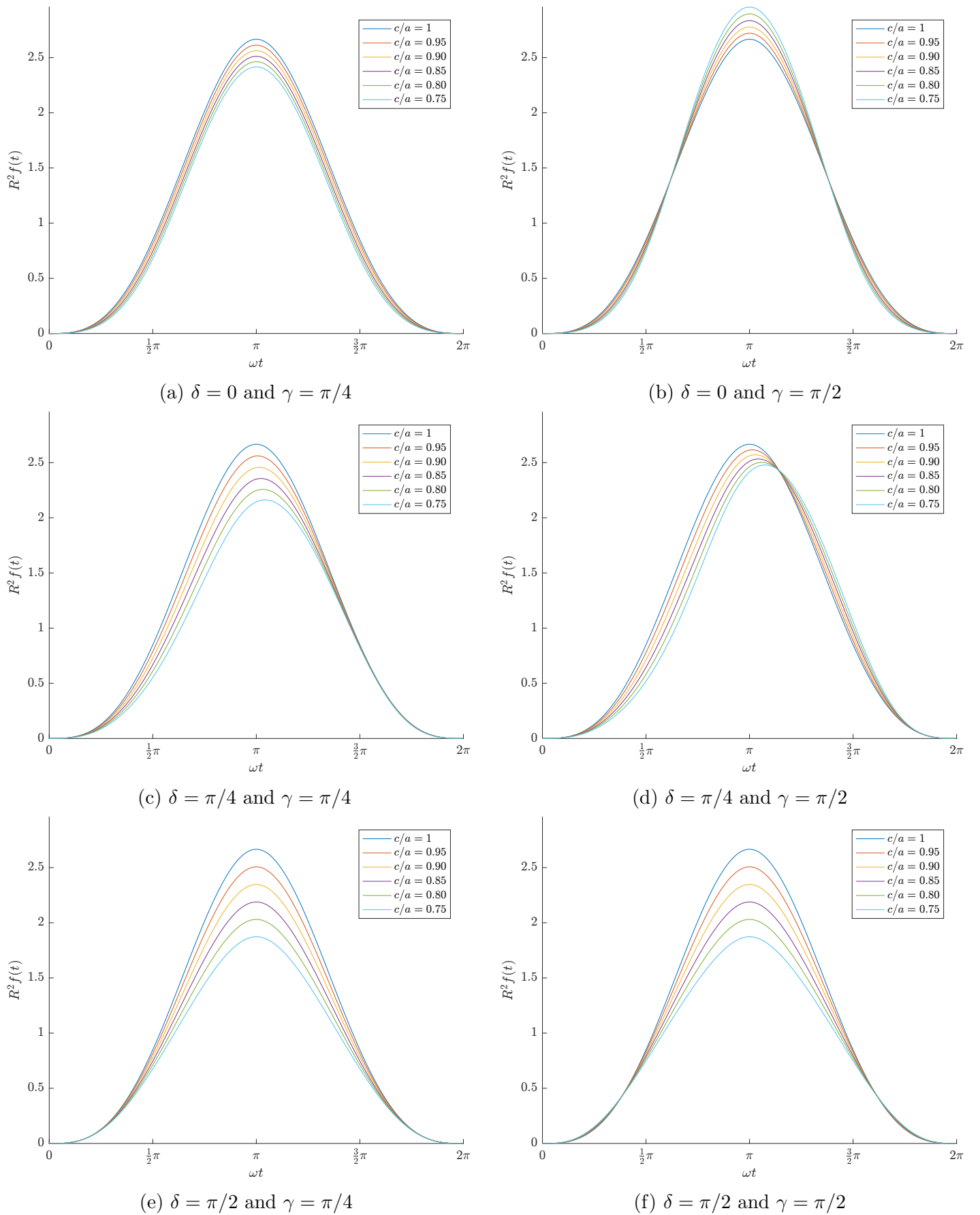
Figure 17: $R^2 f(t)$ against β of spheroids ranging from $c/a = 1$, a sphere, to $c/a = 0.75$ at edge-on observation for some tilts.

In figure 17 we notice that

1. the light-curve of the sphere, for which $(c/a = 1)$, is invariant to any rotation as argued.

2. the maximum values of the light-curve are spread out the most the greater the value of δ on the interval $0 \leq \delta \leq \pi/2$.

3. only for $\delta = 0$ and $\delta = \pi/2$ the light-curve is symmetrical around $\beta = \pi$ at which the light-curves have their maxima. For $0 < \delta < \pi/2$, the light-curves are not symmetrical around $\beta = \pi$ as shown for $\delta = \pi/4$.

4. the light-curves become more sharply peaked around the maximum for increasing γ on the interval $0 \leq \gamma \leq \pi/2$.

5. the maxima of the light-curves decrease with δ on the interval $0 \leq \delta \leq \pi/2$ and increase with γ on the interval $0 \leq \gamma \leq \pi/2$. This can be explained as with increasing γ on the interval $0 \leq \gamma \leq \pi/2$, the thicker side of the ellipsoid is rotated in the direction of the observer. For increasing δ on the interval $0 \leq \delta \leq \pi/2$, the thicker side of the planet gets rotated away from the integration domain when the integration domain is at its peak at $\beta = \pi$. This explains the lower maxima and the aforementioned offset maxima.

6. only for $\delta = 0$ and $\gamma = \pi/2$, the maxima of the light-curves go from high to low with increasing c/a. This is because at $\delta = 0$ and $\gamma = \pi/2$, the largest possible area of the spheroid is illuminated. Even though the spheroids are smaller for smaller c/a, they are flatter so that a greater percentage of the light is reflected towards the observer. This effect is so dominant, that every planet with equal c has a light-curve with a maximum above that of a sphere if $c/a < 1$ at $\delta = 0$ and $\gamma = \pi/2$

As we did in the case of a solar system triaxially-shaped dwarf planet, we will now look at the Fourier coefficients of the light-curve. We are going to calculate the Fourier coefficients of the light-curve for any given tilt in order to determine if we can determine the tilt of a given planet with its Fourier coefficients. In figure 18 we show the Fourier coefficients $a_0...a_2$, a_4, b_1, b_2 and b_4 for edge-on observation for all possible tilts. The Fourier coefficients a_3 and b_3 were left out due to their small values (10^{-10}). Note that the axes all have different scales.

(a) a_0

(b) a_1

(c) b_1

(d) a_2

(e) b_2

(f) a_4

(g) b_4
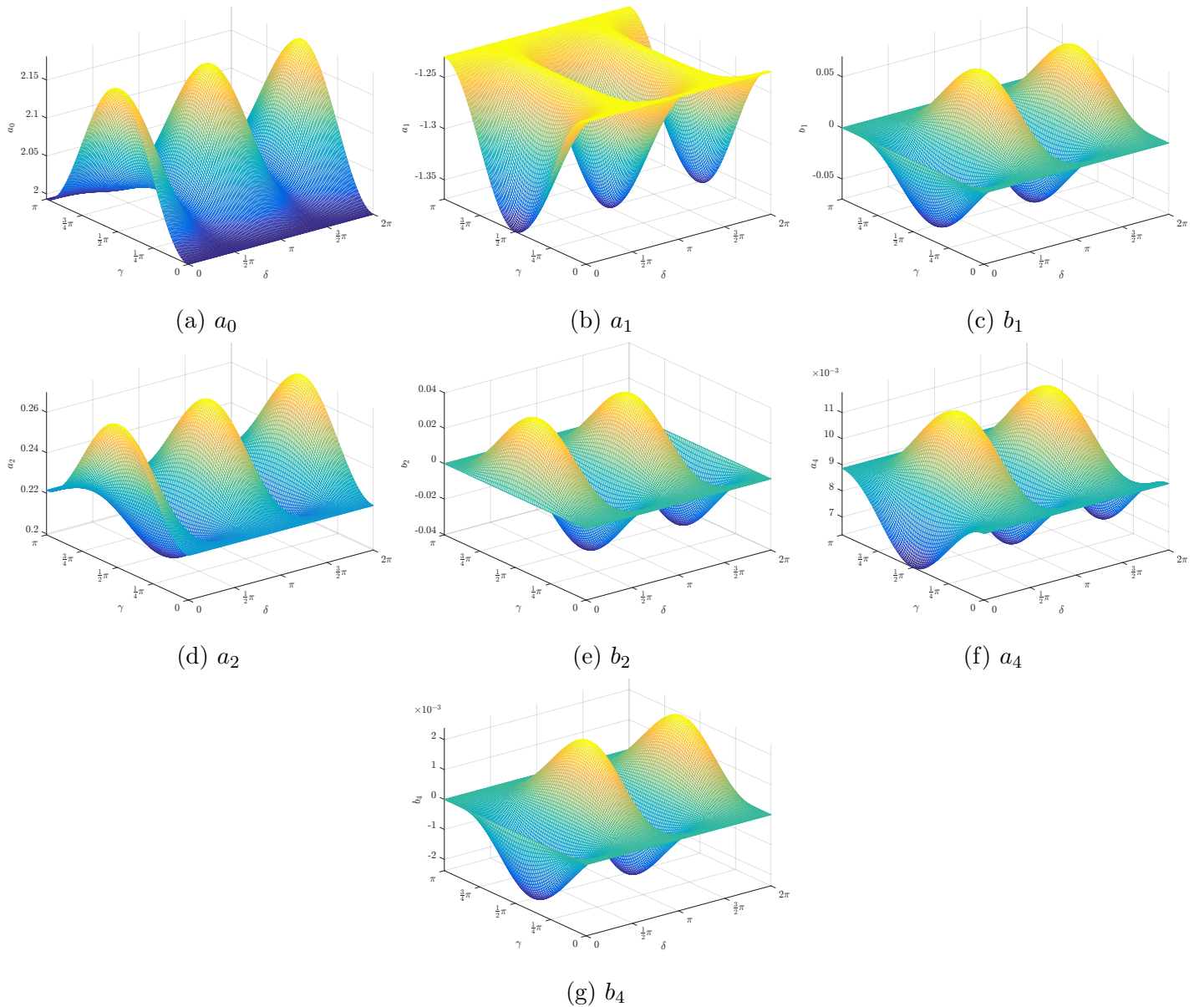
Figure 18: The Fourier coefficients $a_0...a_2, a_4, b_1, b_2$ and b_4 of equation 6 of a spheroidally-shaped exoplanet with the same ratio $a : b : c = 1 : 1 : 0.935$ as Saturn [27] at edge-on observation for all possible tilts. Note that the axes all have different scales.

In figure 18 we notice that

1. $b_1...b_4$ are zero for $\gamma = 0$ and for $\gamma = \pi$. This is because at $\gamma = 0$ and $\gamma = \pi$, the planet has no tilt so that the light-curve is symmetrical around $\beta = \pi$.

2. all the Fourier coefficients are symmetric around $\gamma = \pi/2$. This was already argued when we considered the symmetries of a spheroidally-shaped exoplanet at edge-on observation to find out for which tilts the light-curves are indistinguishable from each other.

3. the Fourier coefficients $a_0...a_2$ are symmetric around $\delta = \pi$ and the other Fourier coefficients have the same values for δ as they do for $\delta + \pi$. This was already argued, that the light-curves and therefore the Fourier coefficients have the same values for $\pi \leq \delta < 2\pi$ as they have for $0 \leq \delta \leq \pi$.

4. we generally can only detect $a_0...a_2$, a_4, b_1 and b_4 as all the other Fourier coefficients have a smaller amplitude then $10^{-3}a_0$.

28

5. given a measured light-curve, the measurable Fourier coefficients do not give enough information to determine the tilt. This is because most values for each Fourier coefficient corresponds to multiple possible tilts. The Fourier coefficients $a_0...a_2$ all give the same curves of possible tilts. So do the Fourier coefficients a_4, b_1 and b_4. This is due to the aforementioned symmetries in δ. If at least one Fourier coefficient of both of the sets $a_0...a_2$ and a_4, b_1 and b_4 are known, we can narrow the possible tilt down to a finite amount of values. However, we cannot narrow the possible tilt down to a single value, due to our assumption that planets are homogeneous. That assumption eliminates the possibility to distinguish between for example a planet without tilt and a planet with $\gamma = \pi$ and $\delta = 0$.

4.4.   Spheroidally-shaped exoplanet with tilt at face-on observation

Now we consider a spheroidally-shaped exoplanet with tilt at face-on observation. As in the case with tilt at edge-on observation, we have to substitute A in equation 5 with $A_{jk} = R_{\mathbf{k}}(\delta)R_{\mathbf{j}}(\gamma)AR_{\mathbf{j}}(\gamma)^T R_{\mathbf{k}}(\delta)^T$ with the rotation matrices $R_{\mathbf{j}}(\gamma)$ and $R_{\mathbf{k}}(\delta)$ given by equation 9. With $|A_{jk}| = |A|$ and everything else the same as in the case without tilt at face-on observation, the light-curve given by equation 5 with tilt at face-on observation becomes

$$f(t) = -\frac{4(abc)^2}{\pi R^2} \int\int_{\mathbb{D}} \frac{\cos\theta \sin^2\theta \cos(\beta - \phi)}{\left|A_{jk}^{-1/2}\hat{\mathbf{u}}\right|^4}\mathrm{d}\phi\mathrm{d}\theta,$$

where the integration domain is $\mathbb{D} = \{(\phi, \theta) : 0 \leq \theta \leq \pi/2, \phi \in \Phi\}$, with

$$\Phi = [\pi/2 + \beta, 3\pi/2 + \beta]$$

is the same as without tilt.

Now we consider the symmetries of a spheroidally-shaped exoplanet at face-on observation to distinguish for which values for γ and δ, the light-curves are distinct. Firstly as in the case of a spheroidally-shaped exoplanet with tilt at edge-on observation, the values of γ that are π apart have the same light-curve. Also, the light-curves for values of δ equidistant to $\delta = 0$ are the same. This is due to the symmetry of the planet along the plane coplanar to $\mathbf{a}$ and $\mathbf{b}$ and because δ is the rotation around the $\mathbf{k}$-axis, which is parallel to the observer for face-on observation.
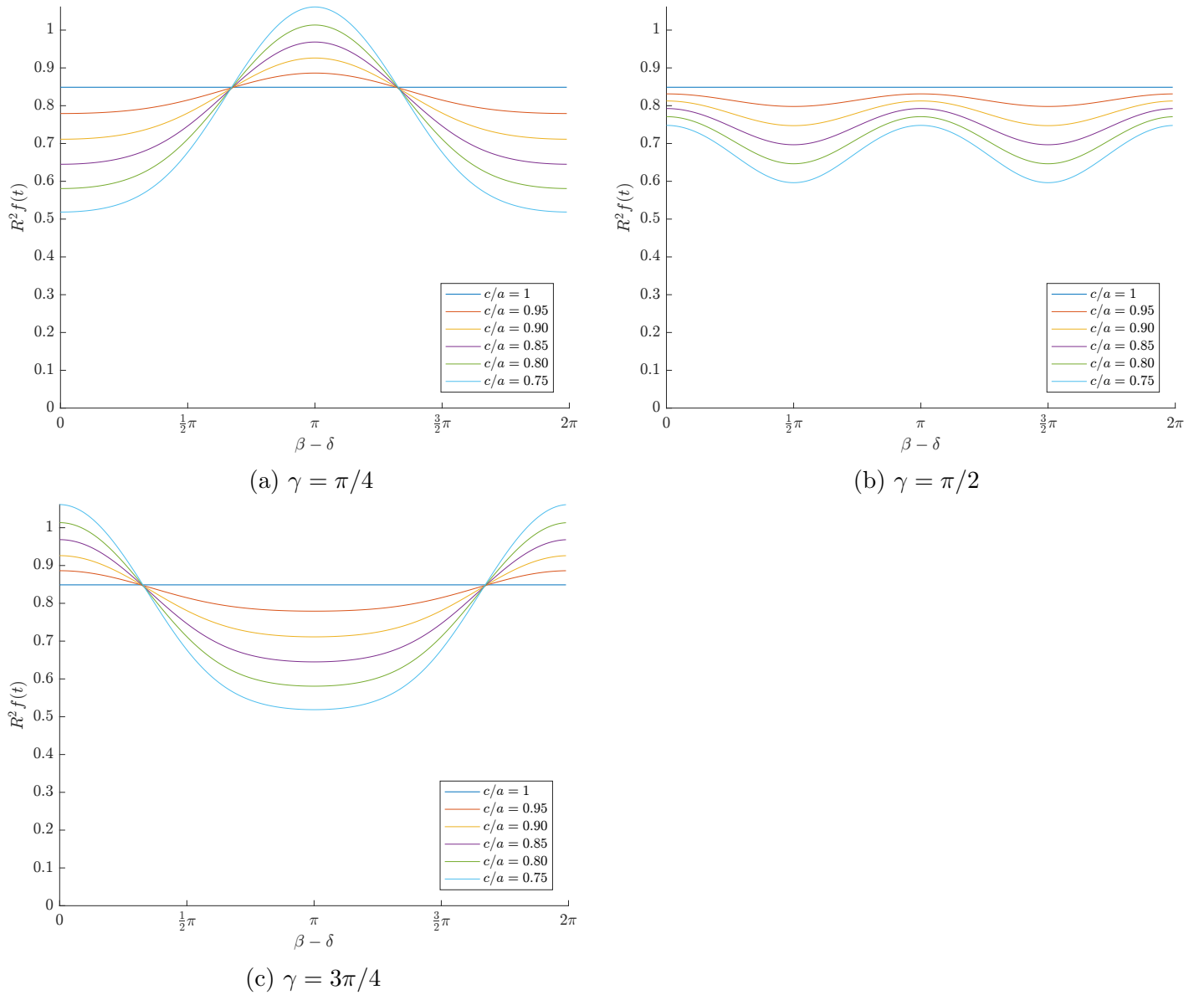
Figure 19: $R^2 f(t)$ against $\beta - \delta$ of spheroids ranging from $c/a = 1$, a sphere, to $c/a = 0.75$ at face-on observation for $\gamma = \pi/4, \pi/2$ and $3\pi/4$.

In figure 19 we show the light-curves for face-on observation for tilts with $0 \leq \gamma < \pi$ and $0 \leq \delta \leq \pi$. As in the case of a spheroidally-shaped exoplanet at edge-on observation, there are no other distinct light-curves due to the aforementioned symmetries. Note that $\gamma = 0$ describes the situation without tilt, which is shown in figure 16.

In figure 19 we notice that

1. as explained in the case of a spheroidally-shaped exoplanet without tilt at edge-on observation, the maxima of the light-curves do exceed the maximum of a spherical planet for various tilts. The maxima for tilts close to $\gamma = \pi/2$ are lower than the maximum of a spherical planet, as the flat side of the planet is then tilted away from the observer.

2. the light-curves for $\delta = 0$ and $\delta = \pi$ are symmetrical around $\beta = \pi$. This is because the planet is still symmetrical in respect to $\mathbf{i}$ for $\delta = 0$ and $\delta = \pi$.

3. the maxima of the light-curves for constant γ shift with the difference of δ.

4. in the case that the maxima of the spheroidally-shaped planets exceed the maximum of the spherically-shaped planet, the maxima of the spheroidally-shaped planets increase for decreasing c/a. In the case that the maximum of the spherically-shaped planet exceed the maxima of the spheroidally-shaped planets, the maxima of the spheroidally-shaped planets decrease for decreasing c/a.

(a) a_0 (b) a_1 (c) b_1

(d) a_2 (e) b_2 (f) a_3

(g) b_3 (h) a_4 (i) b_4
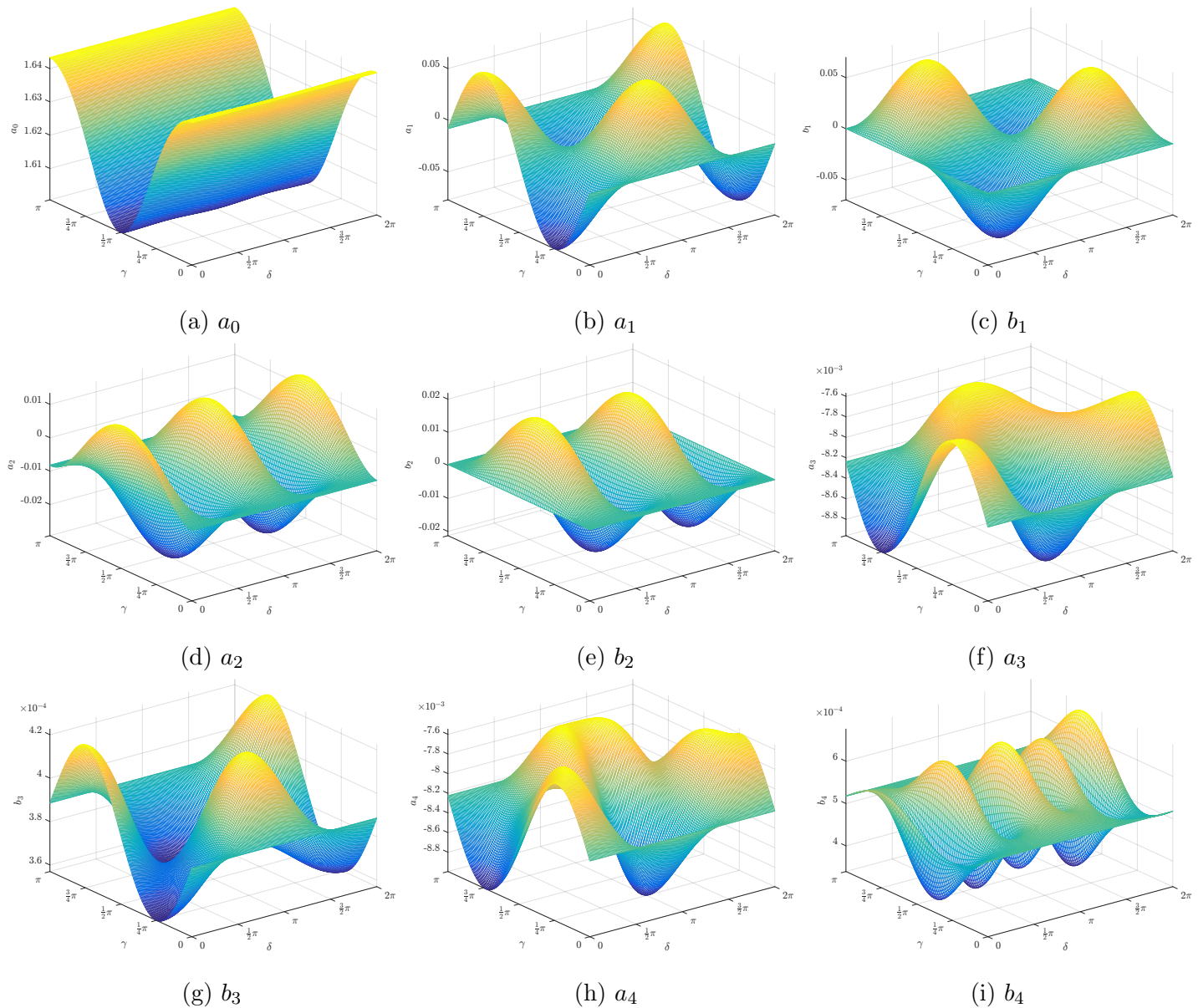
Figure 20: The first 9 Fourier coefficients $a_0...a_4$ and $b_1...b_4$ of equation 6 of a spheroidally-shaped exoplanet with the same ratio $a : b : c = 1 : 1 : 0.935$ as Saturn [27] at face-on observation for all possible tilts. Note that the axes all have different scales.

In figure 20 we show the Fourier coefficients $a_0...a_4$ and $b_1...b_4$ from equation 6. We notice that

1. as explained in the case of a spheroidally-shaped exoplanet at edge-on observation, $b_1...b_4$ are zero for $\gamma = 0$ and $\gamma = \pi$.

2. in this case, unlike the case of edge-on observation, only the Fourier coefficients a_0, a_2 and b_2 are symmetric around $\gamma = \pi/2$.

3. the Fourier coefficients $a_0...a_4$ and b_3 are symmetrical around $\delta = \pi$. The Fourier coefficient b_2 has the same value for δ as for $\delta + \pi$. The Fourier coefficient b_1 has the same value for δ and γ as for $\delta + \pi$ and $\gamma + \pi/2$.

4. a_0 is independent of δ.

5. we can in the case of face-on observation generally only measure $a_0...a_4$, b_1 and b_2.

6. out of the measurable Fourier coefficients, we need to measure at least two Fourier coefficients, with a maximum of one out of $a_0...a_4$, to get a finite amount of possible tilts. Due to the assumption of a homogeneous planet, it is impossible to constrain the actual tilt.

5.   Tidally-locked, triaxially-shaped exoplanet

The final application we consider is a tidally-locked, triaxially-shaped exoplanet. A tidally-locked planet spins around its spin axis in the same amount of time as it rotates around its parent star. For such planets, $\omega = \Omega$, where ω is the angular frequency of the planet orbiting its parent star.

Tidal locking works through torque due to differences in gravitational pull from the parent star between different parts of the planet [29]. With $\mathbf{a}$, the largest of the semi-principal axes, aligned with $\hat{\mathbf{R}}$, the maximum difference in gravitation pull in different parts of the planet is the highest. Therefore we expect more tidally-locked, triaxially-shaped planets with little or no tilt. However, it is possible for a triaxially-shaped planet with tilt to be tidally-locked. There is no example of a tidally-locked planet in our solar system. There are only examples of tidally locked moons, like our own moon. Note that our moon is spheroidally-shaped and not triaxially-shaped. Although there are no examples of tidally-locked planets in our solar system, it is thought there are tidally-locked planets in neighbouring planetary systems. An example of a planet that is thought to be tidally-locked is Alpha Centauri Bb in respect to its parent star Alpha Centauri [29].

Just as in the case of spheroidally-shaped exoplanets, we will consider two possible orientations for the observer to view the exoplanetary system. These orientations are edge-on and face-on. We will also consider all possible orientations the planet can have in respect to the principal axes $\mathbf{i}, \mathbf{j}$ and $\mathbf{k}$. We denote the case with $\hat{\mathbf{a}} = \hat{\mathbf{R}}$ as no tilt. Note that this is not the same definition of no tilt as given in the case of a spheroidally-shaped exoplanet. The alternate definition is necessary here as in this case, we can assume that the planet does not spin.

In section 5.1 we firstly consider the case without tilt at face-on observation. Secondly in section 5.2 we consider the case without tilt at edge-on observation. Then in section 5.3 we consider the case with tilt at edge-on observation. Finally, in section 5.4 we consider the case with tilt at face-on observation.

5.1.   Tidally-locked, triaxially-shaped exoplanet without tilt at face-on observation

In figure 21, we show a tidally-locked, triaxially-shaped exoplanet without tilt in four different locations in its orbit around the star. Notice that $\mathbf{a}, \mathbf{b}, \mathbf{i}$ and $\mathbf{j}$ are coplanar and $\mathbf{c}$, the spin axis, and $\mathbf{k}$, the orbit axis, are parallel. As this is the case without tilt, we notice that $\hat{\mathbf{a}} = \hat{\mathbf{R}}$ throughout its orbit.
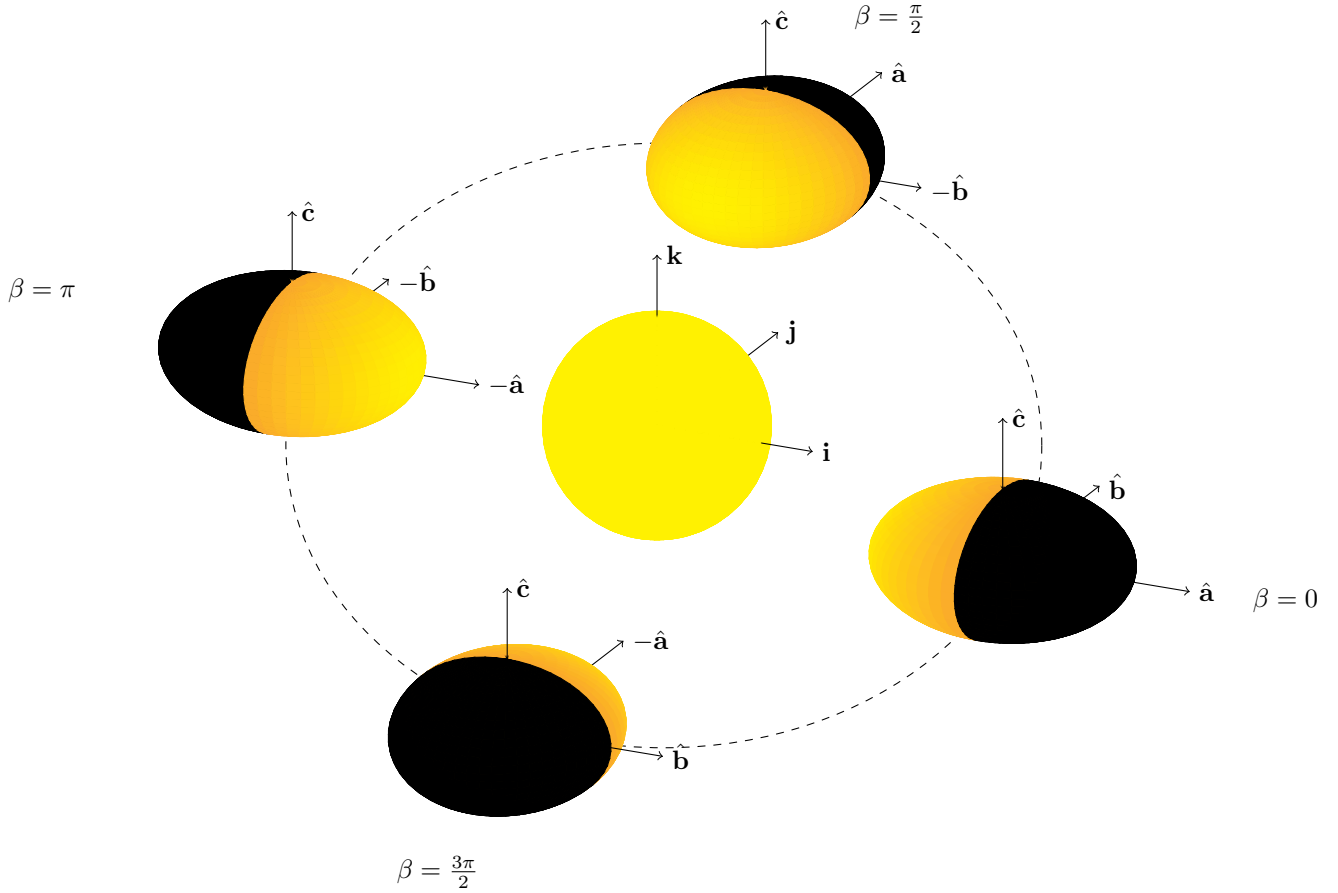
Figure 21: A tidally-locked, triaxially-shaped planet with zero tilt in four different locations in an orbit around its parent star. Due to the tidal locking, $\hat{\mathbf{a}} = \hat{\mathbf{R}}$. Notice that $\mathbf{a}$ and $\mathbf{b}$ are in the orbital plane as the planet has no tilt. Also notice that the spin axis $\mathbf{c}$ and the orbit axis $\mathbf{k}$ are parallel.

For the case without tilt at face-on observation, we expect a flat light-curve. As in the case of a spheroidally-shaped exoplanet at face-on observation, note that $\hat{\mathbf{o}}$ is parallel to the orbit axis around which the orbit of the planet is symmetric. This is true under our assumption of a circular orbit. This symmetry, the assumption that the planet is homogeneous and the fact that the side of the planet that is facing the star is the same throughout the orbit, makes us expect that the light-curve is flat.

To calculate the light-curve given by equation 5, we take $\hat{\mathbf{u}}$ in spherical coördinates in the $(\mathbf{i}, \mathbf{j}, \mathbf{k})$ coordinate system as we did in the case of a spheroidally-shaped exoplanet

$$\hat{\mathbf{u}} = \begin{pmatrix} \cos(\phi)\sin\theta \\ \sin(\phi)\sin\theta \\ \cos\theta \end{pmatrix}.$$

In contrast to the case of a solar system triaxially-shaped dwarf planet, we do not include the spin of the planet in the vector $\hat{\mathbf{u}}$. To take the spin of the planet around its spin axis into account, we denote

$$R_s(\beta) = \begin{pmatrix} \cos\beta & -\sin\beta & 0 \\ \sin\beta & \cos\beta & 0 \\ 0 & 0 & 1 \end{pmatrix}.$$

This is a rotation matrix around the spin axis of the exoplanet without tilt. Because a tidally-locked planet spins around its spin axis in the same amount of time as it rotates around its parent star, the angular

frequency of the spin also is ω. As pointed out in the case of a spheroidally-shaped exoplanet with tilt at edge-on observation, we can take spin into account by substituting A with $A_s = R_s A R_s^T$.
In this manner we can use the same method as with a spheroidally-shaped exoplanet with tilt.

We consider face-on observation for which

$$\hat{\mathbf{o}} = \mathbf{k} = \begin{pmatrix} 0 \\ 0 \\ 1 \end{pmatrix}.$$

As we have assumed that the orbit is circular, we have

$$\hat{\mathbf{R}} = \begin{pmatrix} \cos\beta \\ \sin\beta \\ 0 \end{pmatrix}.$$

In this way, $\hat{\mathbf{R}} = \mathbf{i}$ for $\beta = 0$. To determine the equation for the light-curve given by equation 5, we calculate

$$|A_s| = |A| = (abc)^{-2} \quad \text{and} \quad \mathrm{d}^2\hat{\mathbf{u}} = \sin\theta \mathrm{d}\phi \mathrm{d}\theta. \tag{11}$$

We also have to evaluate the inner products

$$-\hat{\mathbf{R}} \cdot \hat{\mathbf{u}} = -\cos(\phi - \beta)\sin\theta \quad \text{and} \quad \hat{\mathbf{u}} \cdot \hat{\mathbf{o}} = \cos\theta.$$

If we substitute this into equation 5, we get the light-curve

$$f(t) = -\frac{4(abc)^2}{\pi R^2} \int\int_{\mathbb{D}} \frac{\sin^2\theta \cos(\phi - \beta)\cos\theta}{\left|A_s^{-1/2}\hat{\mathbf{u}}\right|^4} \mathrm{d}\phi \mathrm{d}\theta.$$

Now to determine the integration domain, we calculate the terminator

$$\hat{\mathbf{u}} \cdot \hat{\mathbf{o}} = 0 \quad \text{for} \quad \theta = \pi/2.$$

Notice that this inner product does not depend on β at face-on observation, which means that as we expected, the part of the planet that is observed is constant over the entire orbit. We also calculate the limb

$$\hat{\mathbf{R}} \cdot \hat{\mathbf{u}} = 0 \quad \text{for} \quad \phi = \pi/2 + \beta \vee \phi = 3\pi/2 + \beta.$$

From the terminator and the limb we calculate the integration domain

$$\mathbb{D} = \{(\phi, \theta) : 0 \leq \theta \leq \pi/2, \pi/2 + \beta \leq \phi \leq 3\pi/2 + \beta\}.$$

When we calculate this light-curve numerically, we also find the same light-curve as predicted independent of β; the light-intensity is constant.
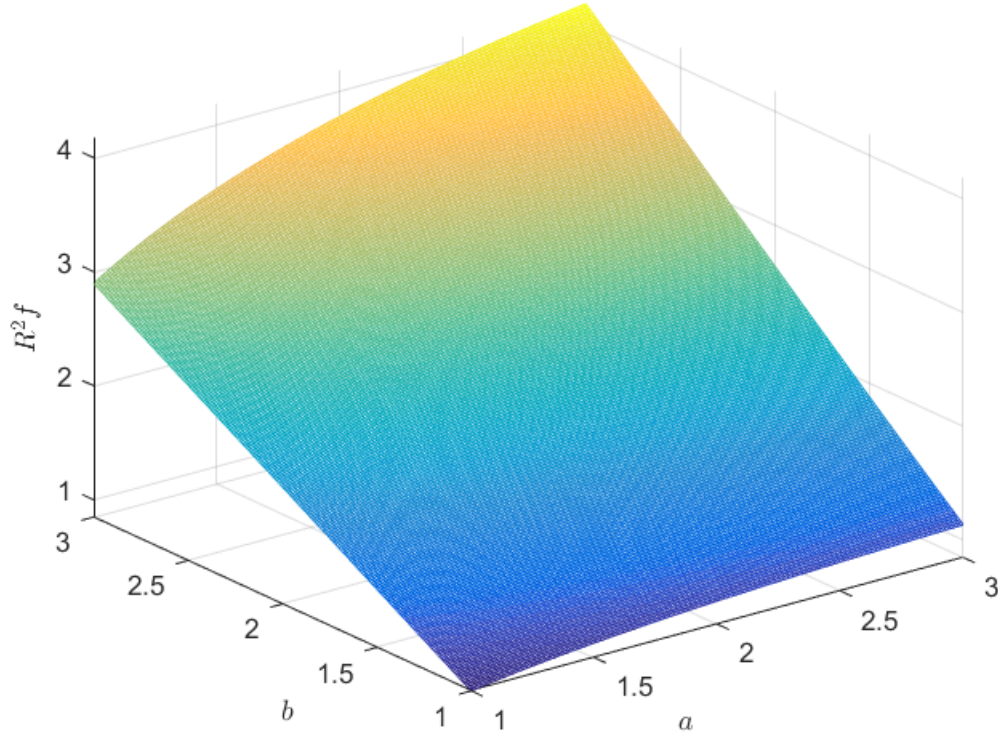
Figure 22: The reflected light-intensity of a tidally-locked, triaxially-shaped exoplanet for $1 \leq a, b \leq 3$ with $c = 1$ without tilt at face-on observation.

The values of this flat light-curve are given in figure 22 for $1 \leq a, b \leq 3$ with $c = 1$. We notice that the values for light-curves of larger planets, i.e. for increasing a and/or increasing b, are consistently larger. We also notice that an increase in b increases the value of the light-curve more than an increase in a. This is due to the fact that $\mathbf{a}$ is aligned with $\hat{\mathbf{R}}$, in contrast to $\mathbf{b}$, which is perpendicular to $\hat{\mathbf{R}}$. Therefore, the cross-section of the planet that intercepts the incident starlight increases with b but not with a.

5.2. Tidally-locked, triaxially-shaped exoplanet without tilt at edge-on observation

Now we consider the case of a tidally-locked, triaxially-shaped exoplanet without tilt at edge-on observation. We use the same method as in the case of face-on observation to calculate the light-curve given by equation 5. The only difference between the edge-on case and the face-on case is that now

$$\hat{\mathbf{o}} = \mathbf{i} = \begin{pmatrix} 1 \\ 0 \\ 0 \end{pmatrix}.$$

This changes the inner product

$$\hat{\mathbf{u}} \cdot \hat{\mathbf{o}} = \cos \phi \sin \theta.$$

As both $\hat{\mathbf{R}}$ and $\hat{\mathbf{u}}$ are the same as with face-on, the terminator is the same. The limb however is different than in the case of edge-on observation

$$\hat{\mathbf{u}} \cdot \hat{\mathbf{o}} = 0 \quad \text{for} \quad \phi = \pi/2 \lor \phi = 3\pi/2.$$

36

This makes the integration domain $\mathbb{D} = \{(\phi, \theta) : 0 \leq \theta \leq \pi, \phi \in \Phi\}$, with

$$\Phi = \begin{cases} [3\pi/2, 3\pi/2 + \beta] & 0 \leq \beta < \pi \\ [\pi/2 + \beta, 5\pi/2] & \pi \leq \beta < 2\pi \end{cases}$$

With $|A_s|$ and $\mathrm{d}^2\hat{\mathbf{u}}$ both the same as in the case of face-on observation, the light-curve of equation 5 is then given by

$$f(t) = -\frac{4(abc)^2}{\pi R^2} \int\int_{\mathbb{D}} \frac{\sin^3\theta \cos\phi \cos(\phi - \beta)}{\left|A_s^{-1/2}\hat{\mathbf{u}}\right|^4} \mathrm{d}\phi\mathrm{d}\theta.$$

This light-curve is shown in figure 23 for various values for a and b and constant c equal to one.
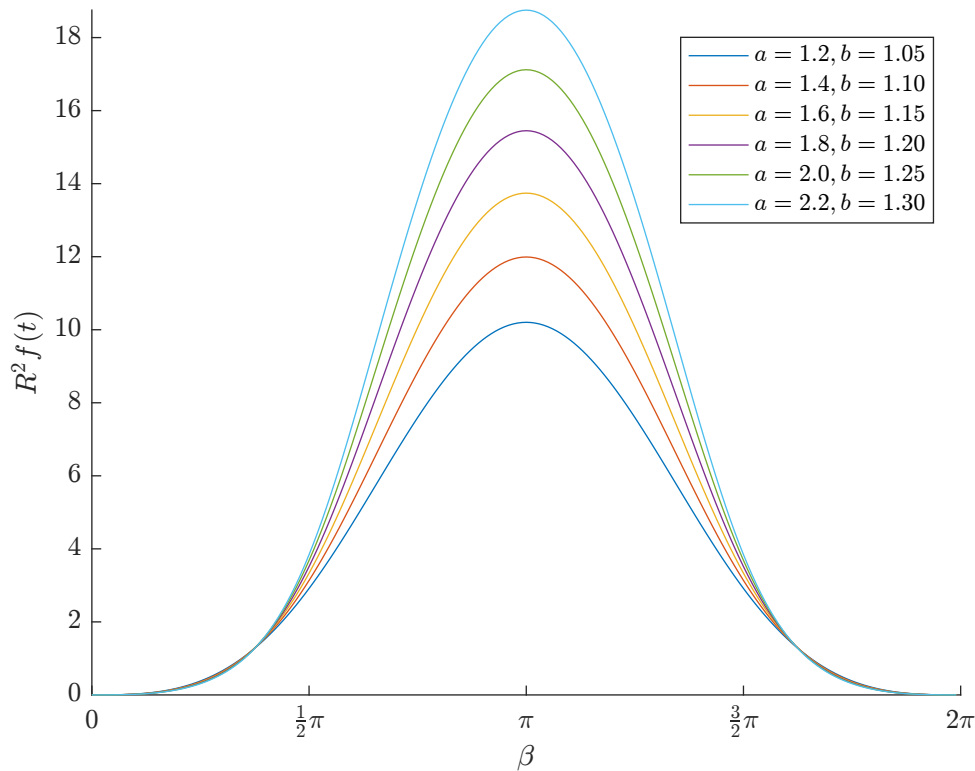
Figure 23: $R^2 f(t)$ against β for tidally-locked, triaxially-shaped exoplanets for several values for a and b with $c = 1$ at edge-on observation.

We notice that the light-curve is symmetrical around $\beta = \pi$, where it has its maximum. This is as expected due to the symmetry of the orbit. The maxima of the light-curves increase with increasing a and b, because the planet is then physically larger. We also notice that the light-curves for the different triaxially-shaped planets are nearly identical for β near $\beta = 0$ and $\beta = 2\pi$. This is because for β near $\beta = 0$, a greater percentage of the light is reflected towards the observer for the smaller a and b. This can make it difficult to determine the shape of a planet with only measurements within a region near $\beta = 0$.

5.3.   Tidally-locked, triaxially-shaped exoplanet at edge-on observation

Now we consider the case of a tidally-locked, triaxially-shaped exoplanet with tilt at edge-on observation. As in the case of a spheroidally-shaped exoplanet with tilt at edge-on observation, we take tilt into account

by substituting A in equation 5. As we already substituted A for A_s to take spin into account, we substitute A in equation 5 with $A_{sjk} = R_{\mathbf{k}}(\delta)R_{\mathbf{j}}(\gamma)A_s R_{\mathbf{j}}(\gamma)^T R_{\mathbf{k}}(\delta)^T$, with the rotation matrices $R_{\mathbf{j}}(\gamma)$ and $R_{\mathbf{k}}(\delta)$ denoted by equation 9. With $|A_{sjk}| = |A|$, the light-curve of equation 5 for a tidally-locked, triaxially-shaped exoplanet with tilt at edge-on observation is given by

$$f(t) = -\frac{4(abc)^2}{\pi R^2} \int \int_{\mathbb{D}} \frac{\sin^3\theta \cos\phi \cos(\phi+\beta)}{\left|A_{sjk}^{-1/2}\hat{\mathbf{u}}\right|^4} \mathrm{d}\phi\mathrm{d}\theta,$$

where the integration domain is the same as without tilt given by $\mathbb{D} = \{(\phi,\theta) : 0 \leq \theta \leq \pi, \phi \in \Phi\}$, with

$$\Phi = \begin{cases} [3\pi/2, 3\pi/2 + \beta] & 0 \leq \beta < \pi \\ [\pi/2 + \beta, 5\pi/2] & \pi \leq \beta < 2\pi \end{cases}.$$

Now we consider the symmetries of a tidally-locked, triaxially-shaped exoplanet at edge-on observation to distinguish the values for γ and δ for which the light-curves are distinct. Firstly, due to edge-on observation and the symmetry of the planet along the plane coplanar with $\mathbf{a}$ and $\mathbf{b}$, the light-curves for γ equidistant to $\gamma = 0$ or $\gamma = \pi$ are the same. Also, light-curves for δ that are π apart are the same due to this symmetry.
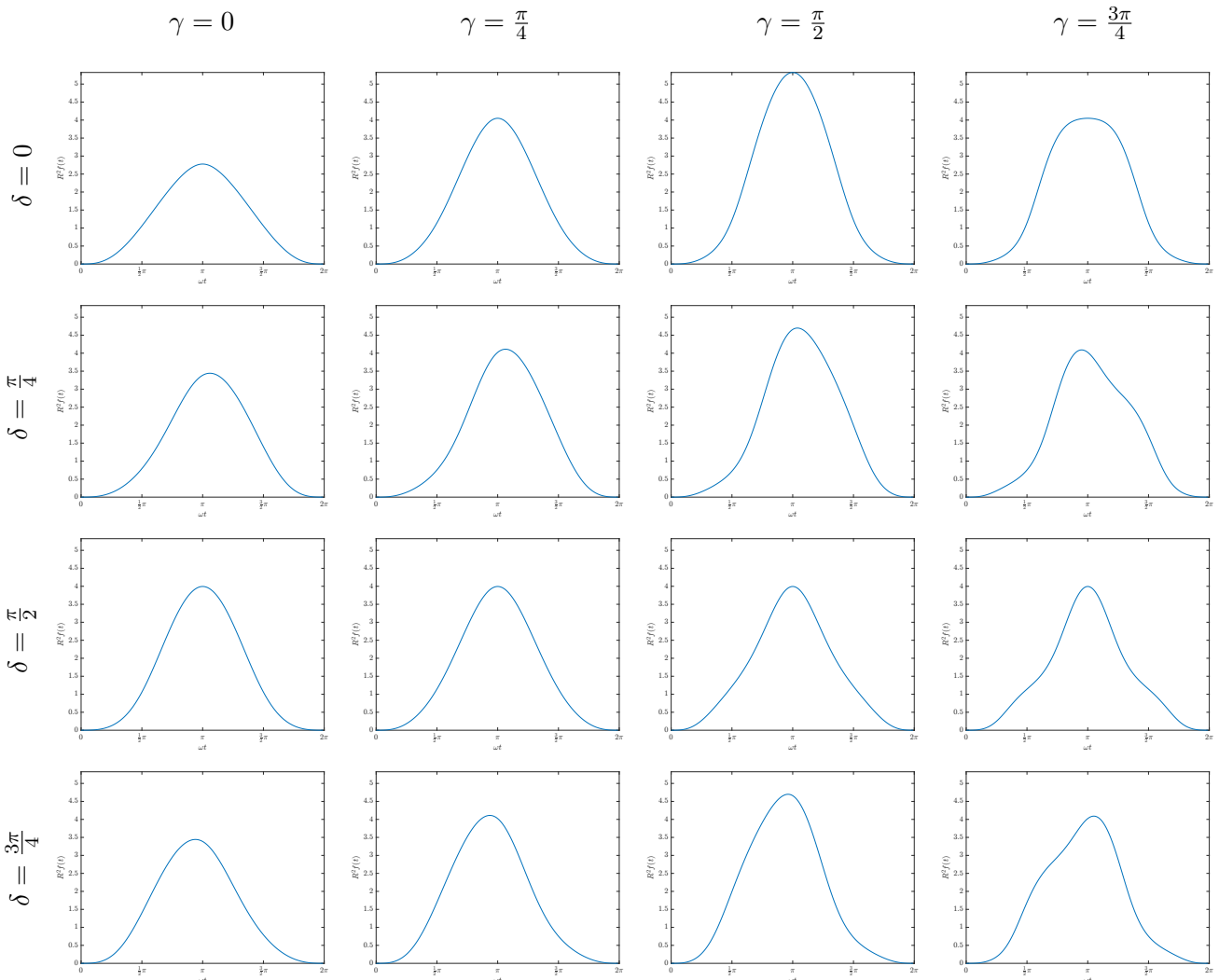
Figure 24: $R^2 f(t)$ against β of a tidally-locked, triaxially-shaped exoplanet with $a : b : c = 1.5 : 1.2 : 1$ at edge-on observation for some tilts.

In figure 24 we show the light-curve of a tidally-locked, triaxially-shaped exoplanet with $a : b : c = 1.5 : 1.2 : 1$ at edge-on observation for tilts with $0 \leq \gamma \leq \pi$ and $0 \leq \delta < \pi$. We notice that

1. only for $\delta = 0$, the light-curves are symmetrical around $\beta = \pi$, where they have their maxima.

2. the light-curves for $\gamma = \pi/2$ have the highest maxima. This is because at $\gamma = \pi/2$, the largest side of the planet is tilted towards the observer. For $\gamma = 0$, the smallest side of the planet is tilted towards the observer resulting into the lowest maxima.

(a) a_0	(b) a_1	(c) b_1
(d) a_2	(e) b_2	(f) a_3
(g) b_3	(h) a_4	(i) b_4
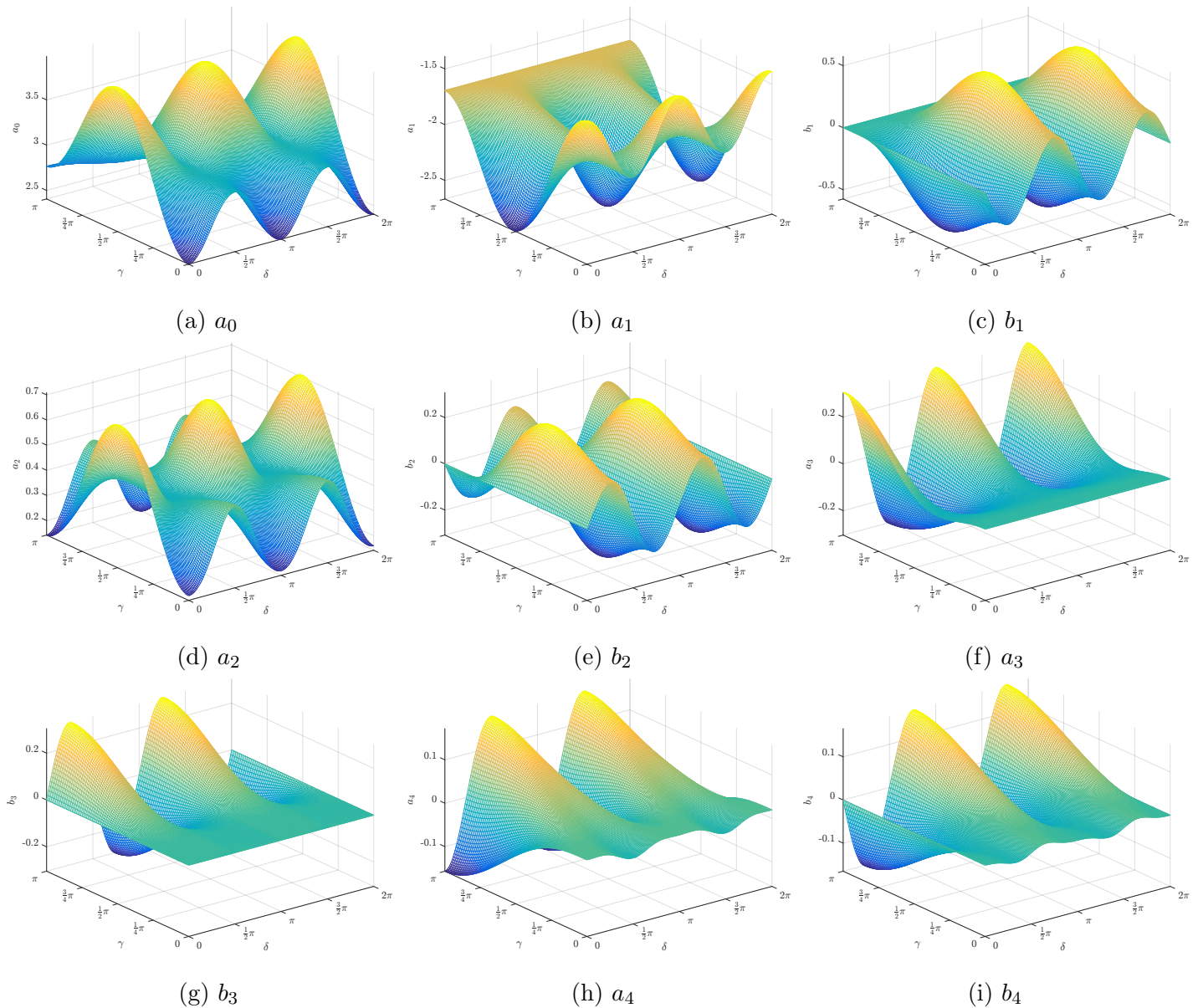
Figure 25: The first 9 Fourier coëfficiënts $a_0...a_4$ and $b_1...b_4$ of equation 6 of a tidally-locked, triaxially-shaped exoplanet with $a : b : c = 1.5 : 1.2 : 1$ at edge-on observation for all possible tilts. Note that the axes all have different scales.

In figure 25 we show the Fourier coefficients $a_0...a_4$ and $b_1...b_4$ from equation 6. We notice that

1. the Fourier coefficients for δ and $\delta + \pi$ are equal, as mentioned when we discussed the symmetries at edge-on observation.

2. these Fourier coefficients are generally measurable as most of the values of the Fourier coefficients are above $10^{-3}a_0$ [25]. Because of this, it is relatively easy to gain a lot of information to determine the tilt accurately.
   We also notice that the Fourier coefficient a_2 is the only Fourier coefficient that is symmetric around $\gamma = \pi/2$.

3. all these Fourier coefficients have other symmetries. Therefore, it is generally sufficient to measure any two of these Fourier coefficients to calculate the tilt. The tilt will never be a single possible tilt, but always either δ or $\delta + \pi$, as those tilts are indistinguishable in our model under the assumption of a homogeneous planet.

5.4.   Tidally-locked, triaxially-shaped exoplanet at face-on observation

Now we consider a tidally-locked, triaxially-shaped exoplanet at face-on observation.

As in the case at edge-on observation, we substitute A in equation 5 with $A_{sjk} = R_{\mathbf{k}}(\delta)R_{\mathbf{j}}(\gamma)A_s R_{\mathbf{j}}(\gamma)^T R_{\mathbf{k}}(\delta)^T$. Here are $R_{\mathbf{j}}(\gamma)$ and $R_{\mathbf{k}}(\delta)$ respectively the rotation matrices around the $\mathbf{j}$-axis and $\mathbf{k}$-axis denoted by equation 9. With $|A_{sjk}| = |A|$, the light-curve given by equation 5 with tilt at face-on observation becomes

$$f(t) = -\frac{4(abc)^2}{\pi R^2} \int \int_{\mathbb{D}} \frac{\sin^2\theta \cos\phi \cos\theta}{\left| A_{sjk}^{-1/2}\hat{\mathbf{u}} \right|^4} \mathrm{d}\phi \mathrm{d}\theta,$$

where the integration domain is again the same as in the case without tilt

$$\mathbb{D} = \{(\phi, \theta) : 0 \le \theta \le \pi/2, \pi/2 + \beta \le \phi \le 3\pi/2 + \beta\}.$$
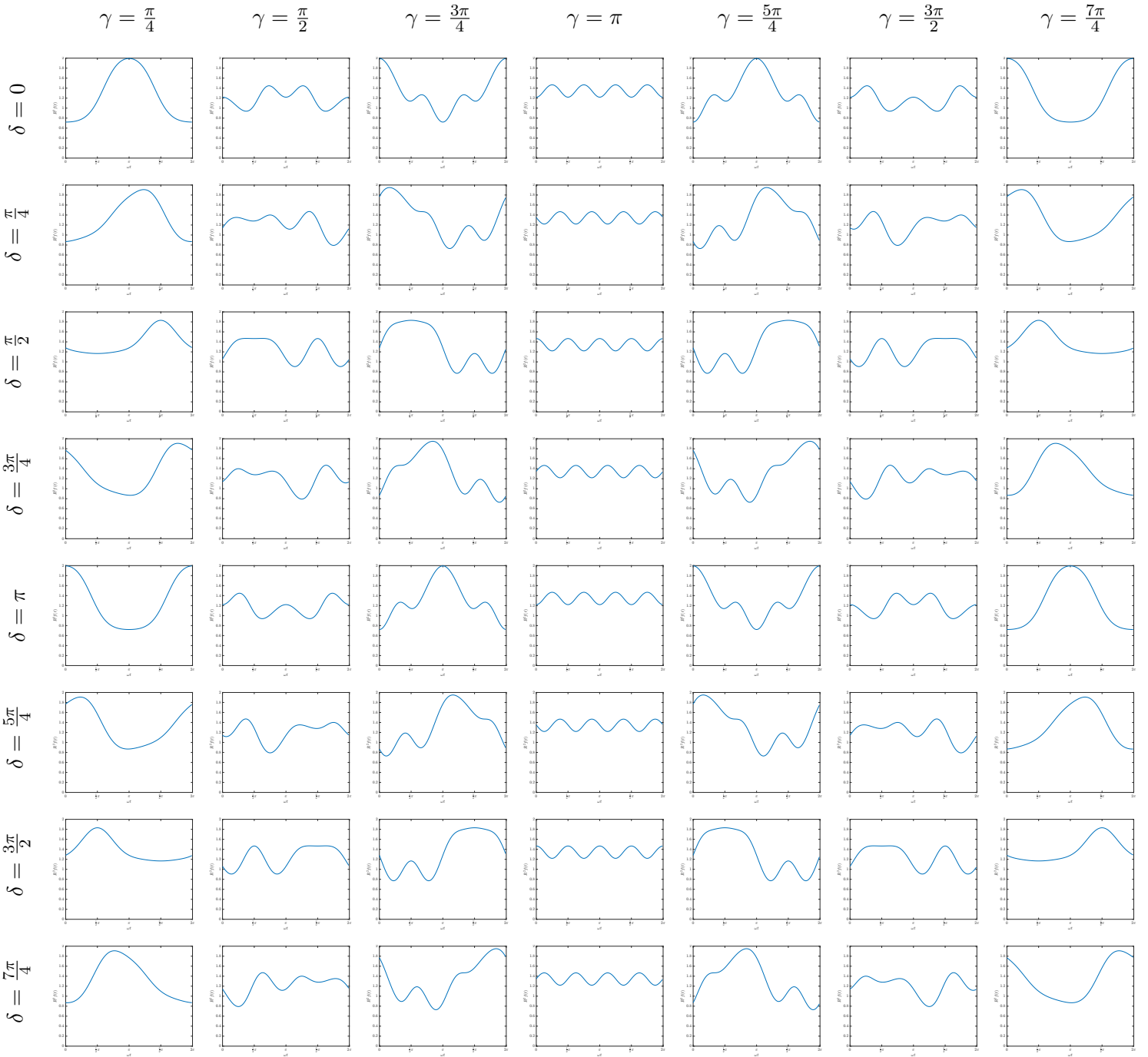
Figure 26: $R^2 f(t)$ against β of a tidally-locked, triaxially-shaped exoplanet with $a : b : c = 1.5 : 1.2 : 1$ at face-on observation for some tilts.

In figure 26 we show the light-curve for face-on observation for all possible tilts. Note that the light-curves for $\gamma = 0$ are those without tilt as shown in figure 22. We notice that

1. for $\gamma = \pi$, the light-curves are identical, except for a phase difference that is equal to the difference in δ.

2. only for $\delta = 0$ and $\delta = \pi$, the light-curves are symmetrical around $\beta = \pi$, due to the symmetry for $\delta = 0$ and $\delta = \pi$.
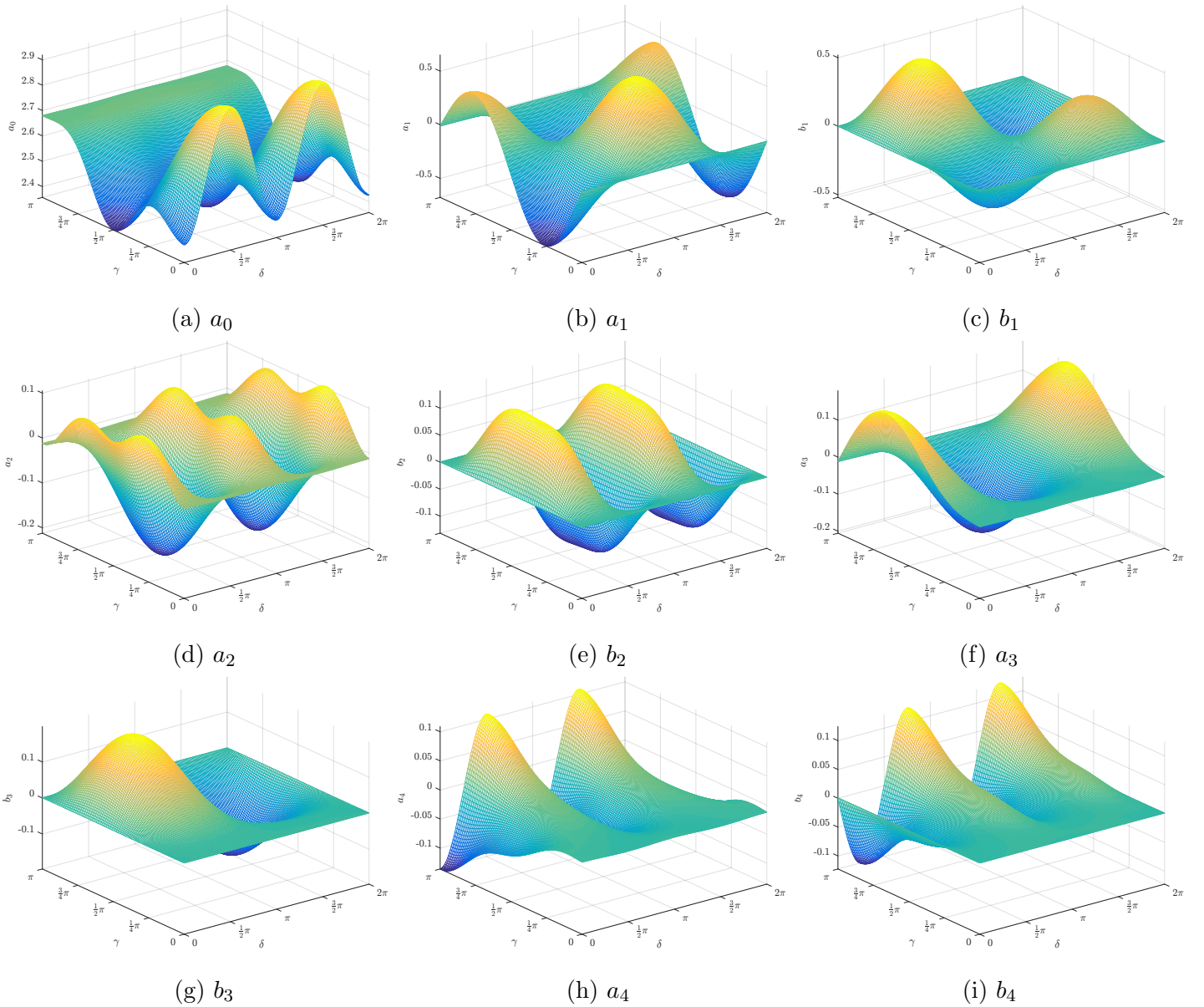
Figure 27: The first 9 Fourier coefficients $a_0...a_4$ and $b_1...b_4$ of equation 6 of a tidally-locked, triaxially-shaped exoplanet with $a : b : c = 1.5 : 1.2 : 1$ at face-on observation for all possible tilts. Note that the axes all have different scales.

In figure 27 we show the Fourier coefficients $a_0...a_4$ and $b_1...b_4$ from equation 6 for the case at face on observation. We notice that the Fourier coefficients $a_0...a_4$ are symmetrical around $\delta = \pi$. We notice that

1. again as in the case at edge-on observation, we can generally measure all these Fourier coefficients as their vales are above $10^{-3}a_0$ for most tilts [25].

2. in contrast to the case of edge-on observation, we can determine the δ if we measure either one of $b_1...b_4$ along with any other Fourier coefficient, as $b_1...b_4$ are not symmetric around $\delta = \pi$. Because apart from the symmetry in δ, all Fourier coefficients have different symmetries, we can measure two Fourier coefficients arbitrarily to derive the tilt.

6.   Conclusion & Discussion

Note that all the figures only show $R^2 f(t)$, never only $f(t)$. Here R is the length of $\mathbf{R}$, the vector from the centre of the parent star to the centre of the planet, and $f(t)$ us the equation for the light-curve. Because our approximation that light-rays follow $\mathbf{R}$, $f(t)/R^2$ does not depend on R. That shows that as argued, the results of this thesis are not limited to a specific orbit type.

Isaac Newton proved in the Principia that a rotating self-gravitating fluid body in equilibrium takes the form of an oblate ellipsoid [3]. In [15] is these spheroids become triaxial for fast spinning planets, called Jacobi ellipsoids. We have calculated the light-curves for ellipsoidally-shaped planets in the cases of a solar system triaxially-shaped dwarf planet, spheroidally-shaped exoplanets and tidally-locked, triaxially-shaped exoplanets.
We assumed that

1. planets are perfect ellipsoids.

2. the planet is in a circular orbit around its parent star.

3. the reflection on the reflective surface of the planet is Lambertian.

4. the reflective surface of the planet is homogeneous with an surface albedo of 1.

5. the starlight that fall on the planet's reflective surface follows $\mathbf{R}$.

6. the starlight reflected off the planet follows $\mathbf{o}$.

7. $\mathbf{o}$ is a constant vector.

With the work of [6], we derived the equation of the light-curves of ellipsoidally-shaped planets.

We have shown that for a solar system triaxially-shaped dwarf planet, the light-curve is a constant plus a cosine with twice the frequency of that of the angular frequency of the planet. We also have shown that this calculated light-curve gives approximately the same light-curve that has been measured for Haumea, which confirms [5].

For spheroidally-shaped exoplanets, we have shown that without tilt, and for edge-on observation, the light-curve differs only by a constant from the light-curve of any other spheroidally-shaped exoplanet. We therefore do not have enough information to differentiate between the flattening and the size of a spheroidally-shaped exoplanet at edge-on observation.
For face-on observation without tilt, we have shown that the light-curve is flat. The value for the light-curve converges to zero as c decreases to zero.
For edge-on observation with tilt, we have shown that for a planet with known dimensions, we can get the tilt up to a factor π in δ, the azimuthal angle of the planetary spin axis, with the measurable Fourier coefficients.
For face-on observation of a planet with known dimensions, we can get the tilt precisely from the Fourier coefficients that can be measured despite intrinsic stellar noise.

For tidally-locked, triaxially-shaped exoplanets, we have shown that without tilt at face-on observation, the light-curve is flat and increasing for increasing a and b for constant c.
For edge-on observation without tilt, we have seen that for different triaxially-shaped exoplanets, the light-curves are nearly identical near $\beta = 0$, with β the orbital phase. If the light-curve is only measured within

this region, it is difficult to determine the shape of the planet.

For edge-on observation with tilt, we have shown that for a planet with known dimensions, we can ascertain the tilt up to a factor π in δ with the measurable Fourier coefficients. These Fourier coefficients are more easily measurable than those of a spheroidally-shaped exoplanet.

For face-on observation with tilt, we have shown that for a planet with known dimensions, we can determine the tilt with the measurable Fourier coefficients. These Fourier coefficients are also more easily measurable than those of a spheroidally-shaped planet.

We have shown in all the applications that we can find the dimensions of the planet with known tilt and that we can find the tilt with known dimensions. We have however not shown how to find the tilt of a spheroidally-shaped or tidally-locked, triaxially-shaped exoplanet without knowing its dimensions. Nor have we shown how to find the dimensions without knowing the tilt.

Therefore, we have not found a way to find both the tilt and the dimensions of a planet other than the numerical approach of comparing the measured light-curve with a dataset of light-curves calculated for every tilt and every feasible dimension. Even then, as shown for a spheroidally-shaped exoplanet without tilt, we do not always get an unique configuration.

References

[1] U. Dyudina, X. Zhang, L. Li, P. Kopparla, A. P. Ingersoll, L. Dones, A. Verbiscer, and Y. L. Yung, "Reflected Light Curves, Spherical and Bond Albedos of Jupiter- and Saturn-like Exoplanets," *apj*, vol. 822, p. 76, May 2016.

[2] C. Armstrong and H. Rein, "High-order harmonics in light curves of Kepler planets," *mnras*, vol. 453, pp. L98–L102, Oct. 2015.

[3] "Reference ellipsoid." `https://en.wikipedia.org/wiki/Reference_ellipsoid`. Version 15 April 2016, at 14:08.

[4] "Jupiter." `https://en.wikipedia.org/wiki/Jupiter`. Version 31 July 2016, at 09:11.

[5] J. S. Alexandra C. Lockwood, Michael E. Brown, "The size and shape of the oblong dwarf planet haumea," *Earth, Moon, and Planets*, pp. 127–137, 2014.

[6] P. Visser, "Tidal-modified glint and double reflection from binary exoplanets.".

[7] "Discoveries of exoplanets." `https://en.wikipedia.org/wiki/Discoveries_of_exoplanets`. Version 11 July 2016, at 20:07.

[8] "Methods of detecting exoplanets." `https://en.wikipedia.org/wiki/Methods_of_detecting_exoplanets`. Version 11 July 2016, at 14:35.

[9] "Catalog exoplanet.eu." `http://exoplanet.eu/catalog`. Updated 16 Juli 2016.

[10] "Planets orbiting around other stars."

[11] "2m1207b." `https://en.wikipedia.org/wiki/2M1207b`. Version 28 May 2016, at 09:13.

[12] "List of nearest exoplanets." `https://en.wikipedia.org/wiki/List_of_nearest_exoplanets`. Version 12 June 2016, at 18:15.

[13] "Light curve." `https://en.wikipedia.org/wiki/Light_curve`. Version 16 March 2016, at 11:35.

[14] "Wolfram alpha." `http://www.wolframalpha.com/`.

[15] S. CHANDRASEKHAR., *Ellipsoidal Figures of Equilibrium*. 10 1987.

[16] "Haumea." `https://en.wikipedia.org/wiki/Haumea`. Version 9 May 2016, at 15:31.

[17] "Planet nine." `https://en.wikipedia.org/wiki/Planet_Nine`. Version 17 July 2016, at 09:35.

[18] "Lambertian reflectance." `https://en.wikipedia.org/wiki/Lambertian_reflectance`. Version 15 April 2016, at 14:08.

[19] "Sun." `https://en.wikipedia.org/wiki/Sun`. Version 20 June 2016, at 05:59.

[20] "Earth." `https://en.wikipedia.org/wiki/Earth`. Version 27 June 2016, at 02:34.

[21] "List of largest exoplanets." `https://en.wikipedia.org/wiki/List_of_largest_exoplanets`. Version 22 June 2016, at 19:40.

[22] "List of exoplanet extremes." `https://en.wikipedia.org/wiki/List_of_exoplanet_extremes`. Version 24 June 2016, at 20:08.

[23] "Matlab 9.0, the mathworks, inc., natick, massachusetts, united states.."

[24] A. Gray, *Modern Differential Geometry of Curves and Surfaces with Mathematica.* CRC Press LLC, second edition ed., 1999.

[25] P. M. Visser and F. J. van de Bult, "Fourier spectra from exoplanets with polar caps and ocean glint," *A&A*, vol. 579, p. A21, July 2015.

[26] J. Stansberry, W. Grundy, M. Brown, D. Cruikshank, J. Spencer, D. Trilling, and J.-L. Margot, *Physical Properties of Kuiper Belt and Centaur Objects: Constraints from the Spitzer Space Telescope*, pp. 161–179. 2008.

[27] P. K. Seidelmann, B. A. Archinal, M. F. A'Hearn, A. Conrad, G. J. Consolmagno, D. Hestroffer, J. L. Hilton, G. A. Krasinsky, G. Neumann, J. Oberst, P. Stooke, E. F. Tedesco, D. J. Tholen, P. C. Thomas, and I. P. Williams, "Report of the iau/iag working group on cartographic coordinates and rotational elements: 2006," *Celestial Mechanics and Dynamical Astronomy*, vol. 98, pp. 155–180, jul 2007.

[28] "Saturn." `https://en.wikipedia.org/wiki/Saturn`. Version 5 August 2016, at 21:24.

[29] "Tidal locking." `https://en.wikipedia.org/wiki/Tidal_locking`. Version 9 May 2016, at 15:31.

7.   Appendix A

In this section we find an equation for the principal curvature constants, κ_1 and κ_2, at a point $\mathbf{s}$ on the ellipsoid surface. This method was contrived by Paul Visser. We will first look at the case were the coördinate system is arbitrary, then we look at the case were the ellipsoid is aligned along the coördinate axis.

We define the orthogonal rotation matrix R so that $R\hat{\mathbf{u}} = \mathbf{k}$ and equivalently $\hat{\mathbf{u}} = R^{-1}\mathbf{k}$. Defining $\hat{\mathbf{u}} = \begin{pmatrix} u_1 & u_2 & u_3 \end{pmatrix}^T$ we get:

$$R = \left(\frac{\hat{\mathbf{u}}\times(\hat{\mathbf{u}}\times\mathbf{k})}{|\hat{\mathbf{u}}\times(\hat{\mathbf{u}}\times\mathbf{k})|} \quad \frac{\hat{\mathbf{u}}\times\mathbf{k}}{|\hat{\mathbf{u}}\times\mathbf{k}|} \quad \hat{\mathbf{u}} \right)^T$$

$$= \frac{1}{u_1^2 + u_2^2} \begin{pmatrix} u_1u_3 & u_2u_3 & u_3^2 - 1 \\ u_2 & -u_1 & 0 \\ u_1 & u_2 & u_3 \end{pmatrix}$$

Because R is an orthogonal matrix, $R^{-1} = R^T$.

We will derive the equation for the principal curvature constants by looking what happens to a infinitesimal displacement from the rotated surface point $R\mathbf{s}$, defining:

$$\begin{pmatrix} x \\ y \\ z \end{pmatrix} = R\mathbf{s} + \begin{pmatrix} dx \\ dy \\ dz \end{pmatrix} \tag{12}$$

As we are interested in the curvature of the ellipsoid, we look at what happens when that point is on the surface of the ellipsoid. That means that the point has to follow the equation:

$$1 = \begin{pmatrix} x \\ y \\ z \end{pmatrix}^T RAR^T \begin{pmatrix} x \\ y \\ z \end{pmatrix} \tag{13}$$

By substituting equation 12 into equation 13, we get the following equation:

$$0 = 2u\,dz + \begin{pmatrix} dx \\ dy \\ dz \end{pmatrix}^T RAR^T \begin{pmatrix} dx \\ dy \\ dz \end{pmatrix}$$

Taking $dz^2 = 0$, because $dz^2 \ll dz$, we get the following equation for dz:

$$dz = \frac{-1}{2u} \begin{pmatrix} dx \\ dy \\ 0 \end{pmatrix}^T RAR^T \begin{pmatrix} dx \\ dy \\ 0 \end{pmatrix}$$

κ_1 and κ_2 are then the eigenvalues of the top left 2x2 matrix of RAR^T/u. The product of the eigenvalues of a matrix is equal to the determinant of said matrix, giving:

$$\kappa_1\kappa_2 = \frac{1}{(u_1^2 + u_2^2)^2\,u^2} \left| \begin{pmatrix} u_1u_3 & u_2u_3 & -1 \\ u_2 & -u_1 & 0 \end{pmatrix} A \begin{pmatrix} u_1u_3 & u_2 \\ u_2u_3 & -u_1 \\ u_3^2 - 1 & 0 \end{pmatrix} \right| \tag{14}$$

Equation 14 gives the general expression for the principal curvature constants. If we look at the case that the ellipsoid is aligned along the coordinate axis, we get:

$$A = \begin{pmatrix} \frac{1}{a^2} & 0 & 0 \\ 0 & \frac{1}{b^2} & 0 \\ 0 & 0 & \frac{1}{c^2} \end{pmatrix}$$

By substituting this matrix A in equation 14, we get:

$$\begin{aligned} \kappa_1 \kappa_2 &= |A| \left(\hat{\mathbf{u}}^T A^{-1} \hat{\mathbf{u}} \right)^2 \\ &= |A| \left(\mathbf{s}^T A^2 \mathbf{s} \right)^{-2} \\ &= \frac{1}{a^2 b^2 c^2} \left(\frac{x^2}{a^4} + \frac{y^2}{b^4} + \frac{z^2}{c^4} \right)^{-2} \end{aligned}$$

8.   Appendix B

The area over which we integrate the light intensity is the intersection of the area that is illuminated and the area that is visible from the observers perspective. Both of those area's are described by the unit surface normal $\hat{\mathbf{u}}$. Because of this, we would like to parametrize the area over which we integrate with the unit surface normal. This method was contrived by Paul Visser.

For the parametrization we need to calculate the Jacobian:

$$s^2 d^2 \hat{\mathbf{s}} = \left| \frac{\partial \mathbf{s}}{\partial \theta} \times \frac{\partial \mathbf{s}}{\partial \phi} \right| d\theta d\phi$$

By taking the definition for $\mathbf{u}$ we get:

$$\begin{aligned}
\mathbf{s} &= A^{-1}\mathbf{u} \\
&= uA^{-1}\hat{\mathbf{u}} \\
&= \frac{A^{-1}\hat{\mathbf{u}}}{|A^{-1/2}\hat{\mathbf{u}}|} \\
&= \frac{A^{-1}\hat{\mathbf{u}}}{\left(\hat{\mathbf{u}}^T A^{-1}\hat{\mathbf{u}}\right)^{-1/2}}
\end{aligned}$$

$$d\mathbf{s} = \frac{\mathbf{k}^T A^{-1}\mathbf{k} - A^{-1}\mathbf{k}\mathbf{k}^T}{\left(\mathbf{k}^T A^{-1}\mathbf{k}\right)^{3/2}} A^{-1} d\hat{\mathbf{u}}$$

By using the equality $R\hat{\mathbf{u}} = \mathbf{k}$ and the same matrix R from Appendix A, we can rewrite the linear transformation from $d\hat{\mathbf{u}}$ to $d\mathbf{s}$ in the following form:

$$\frac{\left| \begin{pmatrix} u_1 u_3 & u_2 u_3 & -1 \\ u_2 & -u_1 & 0 \end{pmatrix} \left(\hat{\mathbf{u}}^T A^{-1}\hat{\mathbf{u}} - A^{-1}\hat{\mathbf{u}}\hat{\mathbf{u}}^T\right) A^{-1} \begin{pmatrix} u_1 u_3 & u_2 \\ u_2 u_3 & -u_1 \\ u_3^2 - 1 & 0 \end{pmatrix} \right|}{\left(u_1^2 + u_2^2\right)^2 \left(\hat{\mathbf{u}}^T A^{-1}\hat{\mathbf{u}}\right)^3}$$

By using the same matrix A as we used in appendix A, we can rewrite this to:

$$\frac{a^2 b^2 c^2}{\left(a^2 u_1^2 + b^2 u_2^2 + c^2 u_3^2\right)^2} = \frac{1}{\kappa_1 \kappa_2}$$

$$\begin{aligned}
s^2 d^2 \hat{\mathbf{s}} &= \frac{d^2 \hat{\mathbf{u}}}{\kappa_1 \kappa_2} \\
&= \frac{d^2 \hat{\mathbf{u}}}{|A| \left(\hat{\mathbf{u}}^T A^{-1}\hat{\mathbf{u}}\right)^2}
\end{aligned}$$

When we look at a spherical shell where $a = b = c = r$ and $d\hat{\mathbf{u}} = \hat{\mathbf{r}}$, we get

$$d^2 \mathbf{s} = r^2 \sin(\theta) d^2 \hat{\mathbf{r}}$$

as we expected it to be.

9.   Appendix C

Here you can find the MATLAB [23] scripts used in this thesis.

9.1.   Solar System triaxially-shaped dwarf planet

The calculation of a_0 and a_2

```matlab
% Initializing functions for the integrands of a_0 and a_2
f0 = @(a,b,c,t) (((a.^2+b.^2).*sin(t).^2 + 2.*c.^2.*cos(t).^2).*a.^2*b.^2 ...
                .*sin(t).^3)./((a.^2.*sin(t).^2+c.^2.*cos(t).^2).^1.5 ...
                .*(b.^2.*sin(t).^2+c.^2.*cos(t).^2).^1.5); % a_0
f2 = @(a,b,c,t) ((b.^2-a.^2).*a.^2.*b.^2.*sin(t).^5)./(2.*(a.^2.*sin(t).^2 ...
                + c.^2.*cos(t).^2).^1.5.*(b.^2.*sin(t).^2+c.^2.*cos(t).^2).^1/5); % a_2

theta = 0:pi/99:pi; % theta from 0 to pi in 100 steps
stepsize = 0.01; % stepsize for the intervals for a and b (with c=1)
interval = 1:stepsize:5; % defining intervals for a and b

% Pre-allocating memory for performance increase
F0 = zeros(length(interval),length(interval)); % Matrix for a_0 for 1<=a,b<=5
F2 = zeros(length(interval),length(interval)); % Matrix for a_2 for 1<=a,b<=5

% Executing 1-dimensional numerical integrals over f0 and f2 for 1<=b<=a<=5
for a = 1:length(interval) % for 1<=a<=5
    for b = 1:a % for 1<=b<=a, as b>a is not considered
        F0(a,b) = trapz(theta,f0(interval(a),interval(b),1,theta)); % Integrating f0
        F2(a,b) = trapz(theta,f2(interval(a),interval(b),1,theta)); % Integrating f2
    end
end
```

Plotting a_0 and a_2 for $1 \le a \le 5$ and $1 \le b \le 5$

```matlab
[R, S] = meshgrid(interval,interval); % Creating grid for the mesh plot for 1<=a,b<=5
F0(F0==0)=nan; % Exempt b>a out of the plot
F2(F2==0)=nan; % Exempt b>a out of the plot

% Plotting a_0
figure % Initializing figure
mesh(R,S,F0); % mesh plot
xlabel('$b$','interpreter','latex'); % Label x-axis
ylabel('$a$','interpreter','latex'); % Label y-axis
zlabel('$R^2a_0$','interpreter','latex'); % Label z-axis

% Plotting a_2
figure % Initializing figure
mesh(R,S,F2); % mesh plot
xlabel('$b$','interpreter','latex'); % Label x-axis
ylabel('$a$','interpreter','latex'); % Label y-axis
zlabel('$R^2a_2$','interpreter','latex'); % Label z-axis
```

Plotting the example Haumea

```matlab
a = 1.94; b = 1.56; c = 1; % Defining ratios of Haumea
a = find(a==interval); % Finding at which place a is in interval
b = find(b==interval); % Finding at which place b is in interval
wt = 0:0.001:2*pi; % Omega*t from 0 to 2*pi (an entire rotation) in steps of 0.001

% Plotting the light-curve for Haumea
figure % Initializing figure
axis([0 2*pi 3.2 5]) % Show x-axis for [0,2*pi] and y-axis for [3.2,5]
set(gca,'xtick',0:0.5*pi:2*pi) % Set markings x-axis to multiples of pi/2
set(gca,'TickLabelInterpreter','latex') % Set text compiler to LaTeX
% Assign proper names to the marking on the x-axis in LaTeX
set(gca,'xticklabel',{'$0$','$\frac{1}{2}\pi$','$\pi$','$\frac{3}{2}\pi$','$2\pi$'})

plot(time,F0(a,b)+F2(a,b).*2.*cos(2*wt),'b'); % Plot the light-curve
xlabel('$\Omega t$','interpreter','latex'); % Label x-axis
ylabel('$R^2f(t)$','interpreter','latex'); % Label y-axis
```

9.2.   Spheroidally-shaped exoplanet

Inserting formula light-curve into a MATLAB [23] function

```matlab
syms a b c alpha beta delta gamma phi theta % Create symbolic variables

% Defining all vectors and matrices
Rj  = [cos(gamma) 0 sin(gamma); 0 1 0; -sin(gamma) 0 cos(gamma)]; % Define rotation matrix R_j
Rk  = [cos(delta) -sin(delta) 0; sin(delta) cos(delta) 0; 0 0 1]; % Define rotation matrix R_k

u = [cos(phi).*sin(theta); sin(phi).*sin(theta); cos(theta)]; % Define u
A = [a.^-2 0 0; 0 b^-2 0; 0 0 c^-2]; % Define A
R = [cos(beta); sin(beta); 0]; % Define R
o = [1; 0; 0]; % Define o in case of edge-on observation (warning: comment face-on)
% o = [0; 0; 1]; % Define o in case of face-on observation

A = Rk*Rj*A^(-(1/2))*Rj.'*Rk.'; % A^-1/2 rotated around the j-axis first and then the k-axis
% Note that due to the orthogonality of the rotation matrices and the diagonality of A,
% we can rotate A^-1/2, instead of rotating A first and then raise to the power -1/2.
% Failing to do so can result into a 16 fold duration increase in calculations.

% Combining eveything into the equation for the light-curve
fI = 4./pi.*a.^2.*b.^2.*c.^2.*sin(theta).*(-R.'*u).*(u.'*o).*sum((A*u).^2).^-2; % Light-curve
f = matlabFunction(fI); % Converting a symbolic function into a numerical function
```

Executing the integrals of the light-curve

```matlab
a = 1; b = 1; % Fix a=b=1 and vary c
beta = 0:pi/100:2*pi-pi/100; % Define beta for [0,2*pi) in 200 steps

fb = zeros(8,8,20,200); % Pre-allocating memory for performance increase for the light-curve
% In order: fb(8 values for delta, 8 values for gamma, 20 values for c, 200 values for beta)

w = waitbar(0,'Starting parallel pool...'); % Initializing waitbar due to the duration of
% this script (Can take up to 4 hours for a i7-6700HQ)
parpool % Initialize for parallel programming
tic % Start timer
waitbar(0,w,'First iteration...'); % Update waitbar

for l = 1:8 % for 8 values of delta
    delta = (l-1)*pi/4; % delta for all possible multiples of pi/4
    for k = 1:8 % for 8 values of gamma
        gamma = (k-1)*pi/4; % gamma for all possible multiples of pi/4
        for j = 1:20 % for 20 values of c
            c = 1-(j-1)*0.05; % c=1 till c=0.05 in steps of 0.05
            parfor i = 1:200 % for 200 values of beta
                fp = @(phi,theta) f(a,b,beta(i),c,delta,gamma,phi,theta);
                if (i<101) % for beta in [0,pi] with corresponding integration areas
                    % Numerical integration over theta and phi for edge-on observation
                    fb(l,k,j,i) = integral2(fp,3*pi/2,3*pi/2+beta(i),0,pi); %
                    % Numerical integration over theta and phi for face-on observation
                    fb(l,k,j,i) = integral2(fp,pi/2+beta(i),3*pi/2+beta(i),0,pi/2);
                    % Warning: choose one
                else % for beta in (pi,2*pi) with corresponding integration areas
                    % Numerical integration over theta and phi for edge-on observation
                    fb(l,k,j,i) = integral2(fp,-3*pi/2+beta(i),pi/2,0,pi);
                    % Numerical integration over theta and phi for face-on observation
                    fb(l,k,j,i) = integral2(fp,pi/2+beta(i),3*pi/2+beta(i),0,pi/2);
```

```matlab
                    % Warning: choose one
                end
            end
        end

        % Updating waitbar
        t1 = toc; % Current running time in seconds
        h_dur = floor(t1/3600); % Amount of hours,
        m_dur = floor((t1-3600*h_dur)/60); % minutes
        s_dur = floor(t1-h_dur*3600-m_dur*60); % and seconds the script has run
        t2 = t1*64/(8*(l-1)+k)-t1; % Predicting time left
        h_est = floor(t2/3600); % Amount of hours,
        m_est = floor((t2-3600*h_est)/60); % minutes
        s_est = floor(t2-h_est*3600-m_est*60); % and seconds the script is predicting to run
        cl = clock; % Request current time
        % Estimated time the script will finish in
        h_end = mod(cl(4)+h_est+floor((cl(5)+m_est+floor((cl(6)+s_est)/60))/60),24); % hours,
        m_end = mod(cl(5)+m_est+floor((cl(6)+s_est)/60),60); % minutes
        s_end = floor(mod(cl(6)+s_est,60)); % and seconds

        % Updating waitbar; displaying at which value of delta and gamma it is currently
        % running, giving the running time and the expected finishing time of the script
        waitbar((8*(l-1)+k)/64,w,sprintf('\\delta=%1.0f\\pi/4 and \\gamma=%1.0f\\pi/4 ...
        at %02d:%02d:%02d, ETA = %02d:%02d:%02d',l-1,k-1,h_dur,m_dur,s_dur,h_end,m_end,s_end));
    end
end
t = toc % Save total running time in seconds
close(w) % Close waitbar
delete(gcp) % Stop parallel processing
```

Plotting the light-curve for several values of the ratio between a and c at edge on observation without tilt

```matlab
h = figure('units','normalized'); % Initializing figure
axis([0 2*pi 0 max(fb(:))]) % Show x-axis for [0,2*pi] and y-axis for [0,max(f(t))]
hold on % multiple plots into one figure
for c = 1:6 % for the first 6 values of c = 0.75:0.05:1
    plot(beta,squeeze(fb(1,1,c,:))); % Plot light-curves for given c
end
legend({'$c/a=1$','$c/a=0.95$','$c/a=0.90$','$c/a=0.85$','$c/a=0.80$','$c/a=0.75$'}, ...
        'interpreter','latex') % Create 6 legend entries for all the plots
xlabel('$\beta$','interpreter','latex') % Label x-axis
ylabel('$R^2f(t)$','interpreter','latex') % Label y-axis
set(gca,'xtick',0:0.5*pi:2*pi) % Set markings x-axis to multiples of pi/2
set(gca,'TickLabelInterpreter','latex') % Set text compiler to LaTeX
set(gca,'xticklabel',{'$0$','$\frac{1}{2}\pi$','$\pi$','$\frac{3}{2}\pi$','$2\pi$'})
% Assign proper names to the markings on the x-axis in LaTeX
```

Plotting the light-curve for several values of the ratio between a and c with tilt

```matlab
for i = 0:2 % delta multiples of pi/2; edge on 0:2, face on 0:4
    for j = 1:2 % gamma multiples of pi/2; edge on 1:2, face on 1:3
        fb(delta+1,gamma+1,1,:) = fb(2,2,1,:); % Copy data of sphere for every tilt
        h = figure('units','normalized'); % Initialize figure
        axis([0 2*pi 0 max(max(max(max(fb(1:3,2:3,2:6,:)))))]) % Show x-axis for [0,2*pi]
        % and y-axis for [0,max(f(t))]
        hold on % multiple plots into one figure
```

```matlab
        for c = 1:6 % for the first 6 values of c = 0.75:0.05:1
            plot(beta,real(squeeze(fb(i+1,j+1,c,:)))); % Plot light-curves for given c
        end
        legend({'$c/a=1$','$c/a=0.95$','$c/a=0.90$','$c/a=0.85$','$c/a=0.80$', ...
                '$c/a=0.75$'},'interpreter','latex') % Create 6 legend entries
        xlabel('$\beta$','interpreter','latex') % Label x-axis
        ylabel('$R^2f(t)$','interpreter','latex') % Label y-axis
        set(gca,'xtick',0:0.5*pi:2*pi) % Set markings x-axis to multiples of pi/2
        set(gca,'TickLabelInterpreter','latex') % Set text compiler to LaTeX
        set(gca,'xticklabel',{'$0$','$\frac{1}{2}\pi$','$\pi$','$\frac{3}{2}\pi$','$2\pi$'})
        % Assign proper names to the markings on the x-axis in LaTeX
    end
end
```

Plotting the light-curve for $\frac{1}{2} \le c \le 1$ at face on observation without tilt

```matlab
a = 1; b = 1; $ Fix a=b=1 and vary c
beta = 0:pi/100:2*pi-pi/100; % Define beta for [0,2*pi) in 200 steps

fb = zeros(51,1); % Pre-allocating memory for performance increase for the light-curve
% In order: fb(201 values for c, 200 values for beta)

parpool % Initialize for parallel programming
tic % Start timer

parfor k = 1:51 % for 51 values of c
    c = 0.5 + (k-1)/100; % c for all possible multiples of 1/100 between 0.5 and 1
    fp = @(phi,theta) f(a,b,0,c,phi,theta); % Inserting known values into the equation of the
    % light-curve so that fp only depends on phi and theta
    fb(k) = integral2(fp,pi/2,3*pi/2,0,pi/2); % Numerical integration over phi between pi/2 and
end

t = toc % Save total running time in seconds

C = 0.5:1/100:1; % Interval of all calculated c's

h = figure('units','normalized'); % Initialize figure
plot(C,fb) % Plot light-curve for all calculated c's
axis([0.5 1 0 1]) % Show x-axis for [0.5,1] and y-axis for [0,1]
xlabel('$c$','interpreter','latex'); % Label x-axis
ylabel('$R^2f(t)$','interpreter','latex') % Label y-axis
```

Executing the integrals of the light-curve for specific c for Fourier analysis

```matlab
a = 1; b = 1; c = 0.935; % Dimensions of Jupiter
beta = 0:pi/100:2*pi-pi/100; % Define beta for [0,2*pi) in 200 steps

fb = zeros(201,201,200); % Pre-allocating memory for performance increase for the light-curve
% In order: fb(201 values for delta, 201 values for gamma, 200 values for beta)

w = waitbar(0,'Starting parallel pool...'); % Initializing waitbar due to the duration of
% this script (Can take up to 4 hours for a i7-6700HQ)
parpool % Initialize for parallel programming
tic % Start timer
waitbar(0,w,'First iteration...'); % Update waitbar

for l = 1:201 % for 201 values of delta
```

```matlab
    delta = (l-1)*pi/100; % delta for all possible multiples of pi/100
    for k = 1:201 % for 201 values of gamma
        gamma = (k-1)*pi/100; % gamma for all possible multiples of pi/100
        parfor i = 1:200 % for 200 values of beta
            fp = @(phi,theta) f(a,b,beta(i),c,delta,gamma,phi,theta);
            if (i<101) % for beta in [0,pi] with corresponding integration areas
                % Numerical integration over theta and phi for edge-on observation
                fb(l,k,i) = integral2(fp,3*pi/2,3*pi/2+beta(i),0,pi); %
                % Numerical integration over theta and phi for face-on observation
                fb(l,k,i) = integral2(fp,pi/2+beta(i),3*pi/2+beta(i),0,pi/2);
                % Warning: choose one
            else % for beta in (pi,2*pi) with corresponding integration areas
                % Numerical integration over theta and phi for edge-on observation
                fb(l,k,i) = integral2(fp,-3*pi/2+beta(i),pi/2,0,pi);
                % Numerical integration over theta and phi for face-on observation
                fb(l,k,i) = integral2(fp,pi/2+beta(i),3*pi/2+beta(i),0,pi/2);
                % Warning: choose one
            end
        end

        % Updating waitbar
        t1 = toc; % Current running time in seconds
        h_dur = floor(t1/3600); % Amount of hours,
        m_dur = floor((t1-3600*h_dur)/60); % minutes
        s_dur = floor(t1-h_dur*3600-m_dur*60); % and seconds the script has run
        t2 = t1*201^2/(201*(l-1)+k)-t1; % Predicting time left
        h_est = floor(t2/3600); % Amount of hours,
        m_est = floor((t2-3600*h_est)/60); % minutes
        s_est = floor(t2-h_est*3600-m_est*60); % and seconds the script is predicting to run
        cl = clock; % Request current time
        % Estimated time the script will finish in
        h_end = mod(cl(4)+h_est+floor((cl(5)+m_est+floor((cl(6)+s_est)/60))/60),24); % hours,
        m_end = mod(cl(5)+m_est+floor((cl(6)+s_est)/60),60); % minutes
        s_end = floor(mod(cl(6)+s_est,60)); % and seconds

        % Updating waitbar; displaying at which value of delta and gamma it is currently
        % running, giving the running time and the expected finishing time of the script
        waitbar((201*(l-1)+k)/201^2,w,sprintf('\\delta=%1.0f\\pi/100 and \\gamma=%1.0f\\pi/100 .
        at %02d:%02d:%02d, ETA = %02d:%02d:%02d',l-1,k-1,h_dur,m_dur,s_dur,h_end,m_end,s_end));
    end
end
t = toc % Save total running time in seconds
close(w) % Close waitbar
delete(gcp) % Stop parallel processing
```

Fourier analysis of the light-curve for specific c

```matlab
coeff = zeros(201,201,9); % Pre-allocating memory for performance increase for the Fourier
% coefficients. In order: coeff(201 values of delta, 201 values of gamma,9 Fourier coefficients)

for delta = 1:201 % for 201 values of delta
    for gamma = 1:201 % for 201 values of gamma
%{a_0%} coeff(delta,gamma,1) = (1/pi)*trapz(beta,fb(delta,gamma,:));
%{a_1%} coeff(delta,gamma,2) = (1/pi)*trapz(beta,squeeze(fb(delta,gamma,:)).*cos(beta)');
%{b_1%} coeff(delta,gamma,3) = (1/pi)*trapz(beta,squeeze(fb(delta,gamma,:)).*sin(beta)');
%{a_2%} coeff(delta,gamma,4) = (1/pi)*trapz(beta,squeeze(fb(delta,gamma,:)).*cos(2*beta)');
%{b_2%} coeff(delta,gamma,5) = (1/pi)*trapz(beta,squeeze(fb(delta,gamma,:)).*sin(2*beta)');
%{a_3%} coeff(delta,gamma,6) = (1/pi)*trapz(beta,squeeze(fb(delta,gamma,:)).*cos(3*beta)');
```

```matlab
%{b_3%}  coeff(delta,gamma,7) = (1/pi)*trapz(beta,squeeze(fb(delta,gamma,:)).*sin(3*beta)');
%{a_4%}  coeff(delta,gamma,8) = (1/pi)*trapz(beta,squeeze(fb(delta,gamma,:)).*cos(4*beta)');
%{b_4%}  coeff(delta,gamma,9) = (1/pi)*trapz(beta,squeeze(fb(delta,gamma,:)).*sin(4*beta)');
    end
end
```

Plotting the Fourier analysis of the light-curve for specific c

```matlab
[X Y] = meshgrid(0:pi/100:2*pi,0:pi/100:2*pi); % Grid for all possible combinations between
% the calculated values of delta and gamma

for i = 1:9 % For the 9 Fourier coefficients
    h = figure('units','normalized'); % Initialize figure
    mesh(X,Y,squeeze(coeff(:,:,i))) % Mesh plot of coefficient i
    axis([0 2*pi 0 2*pi min(min((coeff(:,:,i)))) max(max(coeff(:,:,i)))]) % Show x-axis and
    % y-axis for [0,2*pi] and y-axis for [min(coefficient i),max(coefficient i)]
    xlabel('$\delta$','interpreter','latex'); % Label x-axis
    ylabel('$\gamma$','interpreter','latex') % Label y-axis
    if (i == 1) % If a_0
        zlabel('$a_0$','interpreter','latex') % Label z-axis
    elseif (mod(i,2) == 0) % if a_.
        zlabel(sprintf('$a_%1.0f$',round(i/2)),'interpreter','latex') % Label z-axis
    else % if b_.
        zlabel(sprintf('$b_%1.0f$',floor(i/2)),'interpreter','latex') % Label z-axis
    end

    set(gca,'xtick',0:0.5*pi:2*pi) % Set markings x-axis to multiples of pi/2
    set(gca,'TickLabelInterpreter','latex') % Set text compiler to LaTeX
    set(gca,'xticklabel',{'$0$','$\frac{1}{2}\pi$','$\pi$','$\frac{3}{2}\pi$','$2\pi$'})
    % Assign proper names to the markings on the x-axis in LaTeX
    set(gca,'xtick',0:0.5*pi:2*pi) % Set markings y-axis to multiples of pi/2
    set(gca,'xticklabel',{'$0$','$\frac{1}{2}\pi$','$\pi$','$\frac{3}{2}\pi$','$2\pi$'})
    % Assign proper names to the markings on the y-axis in LaTeX
end
```

9.3.   Tidally locked, triaxially-shaped exoplanets

Inserting formula light-curve into a MATLAB [23] function

```matlab
syms a b c alpha beta delta gamma phi theta % Create symbolic variables

% Defining all vectors and matrices
Rj  = [cos(gamma) 0 sin(gamma); 0 1 0; -sin(gamma) 0 cos(gamma)]; % Define rotation matrix R_j
Rk  = [cos(delta) -sin(delta) 0; sin(delta) cos(delta) 0; 0 0 1]; % Define rotation matrix R_k
Ro = [cos(beta) -sin(beta) 0; sin(beta) cos(beta) 0; 0 0 1]; % Define rotation matrix R_o

u = [cos(phi).*sin(theta); sin(phi).*sin(theta); cos(theta)]; % Define u
A = [a.^-2 0 0; 0 b^-2 0; 0 0 c^-2]; % Define A
R = [cos(beta); sin(beta); 0]; % Define R
o = [1; 0; 0]; % Define o in case of edge-on observation (warning: comment face-on)
% o = [0; 0; 1]; % Define o in case of face-on observation

A = A^-(1/2); % Raise A to the power -1/2
A = Ro*A*Ro.'; % Rotate A around its spin axis k
A = simplify(A); % Simplify A to increase performance
A = Rj*A*Rj.'; % Rotate A around the j-axis
A = simplify(A); % Simplify A to increase performance
A = Rk*A*Rk.'; % Rotate A around the k-axis
A = simplify(A); % Simplify A to increase performance
% Note that due to the orthogonality of the rotation matrices and the diagonality of A,
% we can rotate A^-1/2, instead of rotating A first and then raise to the power -1/2.
% Failing to do so can result into a 16 fold duration increase in calculations.

% Combining eveything into the equation for the light-curve
fI = 4./pi.*a.^2.*b.^2.*c.^2.*sin(theta).*(-R.'*u).*(u.'*o).*sum((A*u).^2).^-2; % Light-curve
f = matlabFunction(fI); % Converting a symbolic function into a numerical function
```

Executing the integrals of the light-curve

```matlab
beta = 0:pi/100:2*pi-pi/100; % Define beta for [0,2*pi) in 200 steps
c = 1; % For fixed c = 1

fb = zeros(8,8,10,200); % Pre-allocating memory for performance increase for the light-curve
% In order: fb(8 values for delta, 8 values for gamma, 10 values for a:b:c, 200 values for beta)

w = waitbar(0,'Starting parallel pool...'); % Initializing waitbar due to the duration of
% this script (Can take up to 4 hours for a i7-6700HQ)
parpool % Initialize for parallel programming
tic % Start timer
waitbar(0,w,'First iteration...'); % Update waitbar

for l = 1:8 % for 8 values of delta
    delta = (l-1)*pi/4; % delta for all possible multiples of pi/4
    for k = 1:8 % for 8 values of gamma
        gamma = (k-1)*pi/4; % gamma for all possible multiples of pi/4
        for j = 1:20 % for 20 values of c
            b = 1 + j/20; a = 4*b - 3*c; % Small Jupiter
            parfor i = 1:200 % for 200 values of beta
                fp = @(phi,theta) f(a,b,beta(i),c,delta,gamma,phi,theta);
                if (i<101) % for beta in [0,pi] with corresponding integration areas
                    % Numerical integration over theta and phi for edge-on observation
                    fb(l,k,j,i) = integral2(fp,3*pi/2,3*pi/2+beta(i),0,pi); %
                    % Numerical integration over theta and phi for face-on observation
```

```matlab
                    fb(l,k,j,i) = integral2(fp,pi/2+beta(i),3*pi/2+beta(i),0,pi/2);
                    % Warning: choose one
                else % for beta in (pi,2*pi) with corresponding integration areas
                    % Numerical integration over theta and phi for edge-on observation
                    fb(l,k,j,i) = integral2(fp,-3*pi/2+beta(i),pi/2,0,pi);
                    % Numerical integration over theta and phi for face-on observation
                    fb(l,k,j,i) = integral2(fp,pi/2+beta(i),3*pi/2+beta(i),0,pi/2);
                    % Warning: choose one
                end
            end
        end

        % Updating waitbar
        t1 = toc; % Current running time in seconds
        h_dur = floor(t1/3600); % Amount of hours,
        m_dur = floor((t1-3600*h_dur)/60); % minutes
        s_dur = floor(t1-h_dur*3600-m_dur*60); % and seconds the script has run
        t2 = t1*64/(8*(l-1)+k)-t1; % Predicting time left
        h_est = floor(t2/3600); % Amount of hours,
        m_est = floor((t2-3600*h_est)/60); % minutes
        s_est = floor(t2-h_est*3600-m_est*60); % and seconds the script is predicting to run
        cl = clock; % Request current time
        % Estimated time the script will finish in
        h_end = mod(cl(4)+h_est+floor((cl(5)+m_est+floor((cl(6)+s_est)/60))/60),24); % hours,
        m_end = mod(cl(5)+m_est+floor((cl(6)+s_est)/60),60); % minutes
        s_end = floor(mod(cl(6)+s_est,60)); % and seconds

        % Updating waitbar; displaying at which value of delta and gamma it is currently
        % running, giving the running time and the expected finishing time of the script
        waitbar((8*(l-1)+k)/64,w,sprintf('\\delta=%1.0f\\pi/4 and \\gamma=%1.0f\\pi/4 ...
        at %02d:%02d:%02d, ETA = %02d:%02d:%02d',l-1,k-1,h_dur,m_dur,s_dur,h_end,m_end,s_end));
    end
end
t = toc % Save total running time in seconds
close(w) % Close waitbar
delete(gcp) % Stop parallel processing
```

Plotting the light-curve for several values of the ratio between a and c without tilt

```matlab
h = figure('units','normalized'); % Initializing figure
axis([0 2*pi 0 max(max(squeeze(fb(1,1,1:6,:))))]) % Show x-axis for [0,2*pi] and y-axis for
% [0,max(light-curves of all a,b)]
hold on % multiple plots into one figure
for c = 1:6 % for the first 6 values of a and b
    plot(beta,squeeze(fb(1,1,c,:))); % Plot light-curves for given a and b
end
legend({'$a=1.2,b=1.05$','$a=1.4,b=1.10$','$a=1.6,b=1.15$','$a=1.8,b=1.20$', ...
        '$a=2.0,b=1.25$','$a=2.2,b=1.30$'},'interpreter','latex') % Create 6 legend entries
xlabel('$\beta$','interpreter','latex') % Label x-axis
ylabel('$R^2f(t)$','interpreter','latex') % Label y-axis
set(gca,'xtick',0:0.5*pi:2*pi) % Set markings x-axis to multiples of pi/2
set(gca,'TickLabelInterpreter','latex') % Set text compiler to LaTeX
set(gca,'xticklabel',{'$0$','$\frac{1}{2}\pi$','$\pi$','$\frac{3}{2}\pi$','$2\pi$'})
% Assign proper names to the marking on the x-axis in LaTeX
```

Plotting the light-curve for several values of the ratio between a and c with tilt

```matlab
for i = 0:4 % delta multiples of pi/2; edge on 0:4, face on 1:7
    for j = 0:3 % gamma multiples of pi/2; edge on 0:3, face on 0:7
        fb(delta+1,gamma+1,1,:) = fb(2,2,1,:); % Copy data of sphere for every tilt
        h = figure('units','normalized'); % Initialize figure
        axis([0 2*pi 0 max(max(max(max(fb(1:3,2:3,2:6,:)))))]) % Show x-axis for [0,2*pi] and
        % y-axis for [0,max(all light-curves)]
        plot(beta,squeeze(fb(i+1,j+1,4,:))); % Plot light-curve
        xlabel('$\beta$','interpreter','latex'); % Label x-axis
        ylabel('$R^2f(t)$','interpreter','latex'); % Label y-axis
        set(gca,'xtick',0:0.5*pi:2*pi) % Set markings x-axis to multiples of pi.2
        set(gca,'TickLabelInterpreter','latex') % Set text compiler to LaTeX
        set(gca,'xticklabel',{'$0$','$\frac{1}{2}\pi$','$\pi$','$\frac{3}{2}\pi$','$2\pi$'})
        % Assign proper names to the markings on the x-axis in LaTeX
    end
end
```

Plotting the light-curve for $1 \leq a, b \leq 3$ at face on observation without tilt

```matlab
fb = zeros(201,201); % Pre-allocating memory for performance increase for the light-curve
% In order: fb(201 values of a, 201 values of b)
parpool % Initialize for parallel programming
tic % Start timer
c = 1; % Fix c = 1

parfor l = 1:201 % for 201 values of a
    a = 1 + (l-1)/100; % Define a
    for k = 1:201 for 201 values of b
        b = 1 + (k-1)/100; % Define b
        fp = @(phi,theta) f(a,b,0,c,phi,theta); % Inserting known values into the equation of
        % the light-curve
        fb(l,k) = integral2(fp,pi/2,3*pi/2,0,pi/2) % Numerical integration over phi between
        % pi/2 and 3*pi/2 and over gamma between 0 and pi/2
    end
end

t = toc % Save total running time in seconds
delete(gcp) % Stop parallel processing

[X Y] = meshgrid(1:0.01:3,1:1/100:3); % Grid for all possible combinations between the
% calculated values of a and b

h = figure('units','normalized'); % Initialize figure
mesh(X,Y,fb') $ Mesh plot of a_0
axis([1 3 1 3 min(fb(:)) max(fb(:))]) % Show x-axis and y-axis for [1,3] and z-axis for
% [min(a_0),max(a_0)]
xlabel('$a$','interpreter','latex'); % Label x-axis
ylabel('$b$','interpreter','latex'); % Label y-axis
zlabel('$R^2f(t)$','interpreter','latex') % Label z-axis
```

Executing the integrals of the light-curve for specific c for Fourier analysis

```matlab
c = 1; b = 1.2; a = 1.5; % Example triaxial
beta = 0:pi/100:2*pi-pi/100; % Define beta for [0,2*pi) in 200 steps

fb = zeros(201,201,200); % Pre-allociting memory for performance increase for the light-curve
```

```matlab
% In order: fb(201 values for delta, 201 values for gamma, 200 values for beta)

w = waitbar(0,'Starting parallel pool...'); % Initializing waitbar due to the duration of
% this script (Can take up to 4 hours for a i7-6700HQ)
parpool % Initialize for parallel programming
tic % Start timer
waitbar(0,w,'First iteration...'); % Update waitbar

for l = 1:201 % for 201 values of delta
    delta = (l-1)*pi/100; % delta for all possible multiples of pi/100
    for k = 1:8 % for 8 values of gamma
        gamma = (k-1)*pi/100; % gamma for all possible multiples of pi/100
        parfor i = 1:200 % for 200 values of beta
            fp = @(phi,theta) f(a,b,beta(i),c,delta,gamma,phi,theta);
            if (i<101) % for beta in [0,pi] with corresponding integration areas
                % Numerical integration over theta and phi for edge-on observation
                fb(l,k,j,i) = integral2(fp,3*pi/2,3*pi/2+beta(i),0,pi); %
                % Numerical integration over theta and phi for face-on observation
                fb(l,k,j,i) = integral2(fp,pi/2+beta(i),3*pi/2+beta(i),0,pi/2);
                % Warning: choose one
            else % for beta in (pi,2*pi) with corresponding integration areas
                % Numerical integration over theta and phi for edge-on observation
                fb(l,k,j,i) = integral2(fp,-3*pi/2+beta(i),pi/2,0,pi);
                % Numerical integration over theta and phi for face-on observation
                fb(l,k,j,i) = integral2(fp,pi/2+beta(i),3*pi/2+beta(i),0,pi/2);
                % Warning: choose one
            end
        end

        % Updating waitbar
        t1 = toc; % Current running time in seconds
        h_dur = floor(t1/3600); % Amount of hours,
        m_dur = floor((t1-3600*h_dur)/60); % minutes
        s_dur = floor(t1-h_dur*3600-m_dur*60); % and seconds the script has run
        t2 = t1*201^2/(201*(l-1)+k)-t1; % Predicting time left
        h_est = floor(t2/3600); % Amount of hours,
        m_est = floor((t2-3600*h_est)/60); % minutes
        s_est = floor(t2-h_est*3600-m_est*60); % and seconds the script is predicting to run
        cl = clock; % Request current time
        % Estimated time the script will finish in
        h_end = mod(cl(4)+h_est+floor((cl(5)+m_est+floor((cl(6)+s_est)/60))/60),24); % hours,
        m_end = mod(cl(5)+m_est+floor((cl(6)+s_est)/60),60); % minutes
        s_end = floor(mod(cl(6)+s_est,60)); % and seconds

        % Updating waitbar; displaying at which value of delta and gamma it is currently
        % running, giving the running time and the expected finishing time of the script
        waitbar((201*(l-1)+k)/201^2,w,sprintf('\\delta=%1.0f\\pi/4 and \\gamma=%1.0f\\pi/4 ...
        at %02d:%02d:%02d, ETA = %02d:%02d:%02d',l-1,k-1,h_dur,m_dur,s_dur,h_end,m_end,s_end));
    end
end
t = toc % Save total running time in seconds
close(w) % Close waitbar
delete(gcp) % Stop parallel processing
```

Fourier analysis of the light-curve for specific c

```matlab
coeff = zeros(201,201,9); % Pre-allocating memory for performance increase for the Fourier
% coefficients
```

```matlab
for delta = 1:201 % for 201 values of delta
    for gamma = 1:201 % for 201 values of gamma
%{a_0%} coeff(delta,gamma,1) = (1/pi)*trapz(beta,fb(delta,gamma,:));
%{a_1%} coeff(delta,gamma,2) = (1/pi)*trapz(beta,squeeze(fb(delta,gamma,:)).*cos(beta)');
%{b_1%} coeff(delta,gamma,3) = (1/pi)*trapz(beta,squeeze(fb(delta,gamma,:)).*sin(beta)');
%{a_2%} coeff(delta,gamma,4) = (1/pi)*trapz(beta,squeeze(fb(delta,gamma,:)).*cos(2*beta)');
%{b_2%} coeff(delta,gamma,5) = (1/pi)*trapz(beta,squeeze(fb(delta,gamma,:)).*sin(2*beta)');
%{a_3%} coeff(delta,gamma,6) = (1/pi)*trapz(beta,squeeze(fb(delta,gamma,:)).*cos(3*beta)');
%{b_3%} coeff(delta,gamma,7) = (1/pi)*trapz(beta,squeeze(fb(delta,gamma,:)).*sin(3*beta)');
%{a_4%} coeff(delta,gamma,8) = (1/pi)*trapz(beta,squeeze(fb(delta,gamma,:)).*cos(4*beta)');
%{b_4%} coeff(delta,gamma,9) = (1/pi)*trapz(beta,squeeze(fb(delta,gamma,:)).*sin(4*beta)');
    end
end
```

Plotting the Fourier analysis of the light-curve for specific c

```matlab
[X Y] = meshgrid(0:pi/100:2*pi,0:pi/100:2*pi); % Grid for all possible combinations between
% the calculated values of delta and gamma

for i = 1:9 % For the 9 Fourier coefficients
    h = figure('units','normalized'); % Initialize figure
    mesh(X,Y,squeeze(coeff(:,:,i))) % Mesh plot of coefficient i
    axis([0 2*pi 0 2*pi min(min((coeff(:,:,i)))) max(max(coeff(:,:,i)))]) % Show x-axis and
    % y-axis for [0,2*pi] and z-axis for [min(coefficient i),max(coefficient i)]
    xlabel('$\delta$','interpreter','latex'); % Label x-axis
    ylabel('$\gamma$','interpreter','latex') % Label y-axis
    if (i == 1) % If a_0
        zlabel('$a_0$','interpreter','latex') % Label z-axis
    elseif (mod(i,2) == 0) % If a_.
        zlabel(sprintf('$a_%1.0f$',round(i/2)),'interpreter','latex') % Label z-axis
    else % If b_.
        zlabel(sprintf('$b_%1.0f$',floor(i/2)),'interpreter','latex') % Label z-axis
    end
    set(gca,'xtick',0:0.5*pi:2*pi) % Set marking x-axis to multiples op pi/2
    set(gca,'TickLabelInterpreter','latex') % Set text compiler to LaTeX
    set(gca,'xticklabel',{'$0$','$\frac{1}{2}\pi$','$\pi$','$\frac{3}{2}\pi$','$2\pi$'})
    % Assign proper names to the markings on the x-axis
    set(gca,'ytick',0:0.5*pi:2*pi) % Set marking y-axis to multiples op pi/2
    set(gca,'yticklabel',{'$0$','$\frac{1}{2}\pi$','$\pi$','$\frac{3}{2}\pi$','$2\pi$'})
    % Assign proper names to the markings on the y-axis
end
```